



Design of a high definition phase retrieval camera for quantum fluids of light

Tangui Aladjidi

Laboratoire Kastler Brossel - Paris

April-June 2020

Contents

Contents	2
1 Introduction	3
2 Theory	5
2.1 What is a quantum fluid of light ?	5
2.2 Correlation measurements	8
2.3 Phase retrieval algorithm	9
3 Numerical simulations	10
3.1 Program structure	11
3.1.1 Image production	12
3.1.2 Phase retrieval	13
3.2 Need for speed : optimization strategies	14
3.3 Performance benchmarks	16
4 Experimental results	20
4.1 Experimental setup	21
4.2 SLM flatness measurement attempts	21
5 Conclusion and outlook	24
References	25
Addendum : Python codes	27

Acknowledgements

I would first like to thank the whole Quantum Optics team who were kind enough to welcome me again. Even with the particular circumstances of the past few months, integration was seamless and allowed for a high productivity in my work even going as far as to ship the necessary equipment to my home ! I also thank warmly Yicheng Wu (main author of [1]) from the Rice University (Houston, USA) for sharing his MATLAB code with me, allowing for much faster progress when porting my code to a GPU impementation.

1 Introduction

Like cold atoms, paraxial fluids of light are a platform that allows to explore many-body quantum particles dynamics. However their beauty resides in the relative simplicity of the experimental setups needed [2]: paraxial fluids of light are generated in hot atomic vapors, using this non-linear and highly tunable medium to generate interactions between photons and thus collective effects such as the emergence of Bogoliubov excitations and superfluidity [3] [4] [5]. The typical setup of such an experiment is presented in fig 1 : a hot atomic vapor of Rubidium (^{85}Rb here) is pumped with a laser tuned near the D_2 line. This generates effective interactions between photons that allow for collective effects such as Bose-Einstein condensation (BEC) and superfluidity [2]. This quantum fluid of light can be characterized using a probe beam, with which one can measure the spectrum of the quantum fluid [3] or create an optical potential [4] on which the fluid will scatter.

In this framework, all of the information about interactions and the properties of the system are encoded in the light field at the output of the atomic vapor cell. It is why retrieval of the intensity and phase of the field would be extremely valuable. This then allows to compute directly many quantities such as correlation functions of the field, giving direct access to the details of the interactions inside of the cell. Measuring correlations as a way to investigate quantum behavior of the system has been proposed to detect exotic effects such as the dynamical Casimir effect [6]. As this will be one of the main topics of the PhD I will follow in the team, setting up this phase retrieval tool could be a critical asset in my future research.

For this purpose, commercially available options already exist for phase retrieval such as Shack-Hartmann sensors [7] or shearing interferometers [8]. However their resolution are limited, overall they offer very low definition (around 400×300 at best) and can be extremely expensive : up to 60000€. The first idea I had on the subject was to build a sort of Michelson interferometer following almost exactly the same setup presented in fig 12, where I would then modulate the phase using the spatial light modulator (SLM) until I extinguished the intensity on the camera (see fig 2). However this "brute force" approach would be quite hard to align, and then brute force search of the extinction would be very slow. Then I found the elegant solution recently presented in [1]. We subsequently decided to try and implement this model.

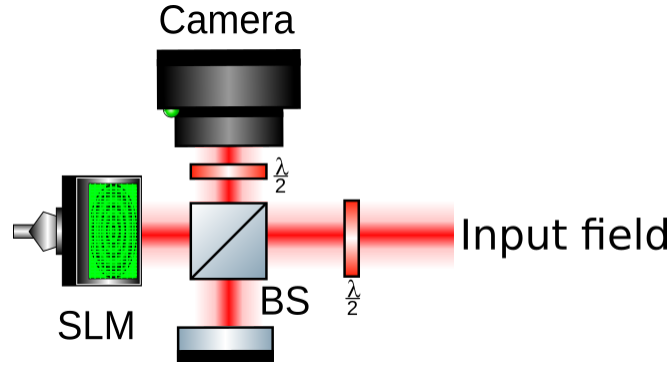


Figure 2: Initial ideal of a modified Michelson interferometer. The input field to characterize is labeled on the right. It is then split by a non polarizing beam splitter (BS). One of the mirrors is replaced by an SLM. Polarization selection is ensured by a half wave plate ($\lambda/2$).

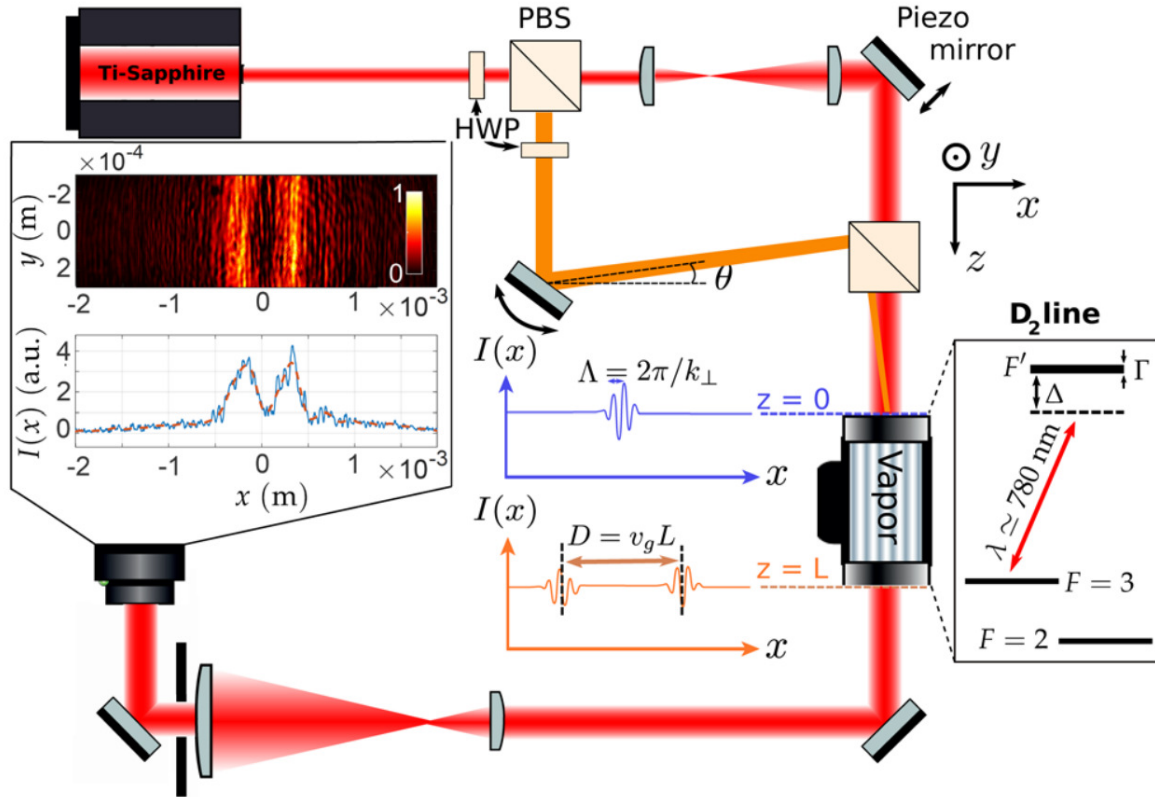


Figure 3: Adapted from [3]. Experimental setup: polarized beam splitter (PBS) and half wave plate (HWP). θ is the angle between the probe (orange beam) and the optical axis defined by the pump (red beam). The probe interferes with the pump and slightly modulates its intensity. (Blue inset) Integrated intensity profile at the input of the medium ($z=0$). The wavelength λ of the density modulation is given by $2\pi/k_{\perp}$, where $k_{\perp} = k_0 \sin \theta$. (Orange inset) Integrated intensity profile at the output of the medium ($z=L$). Here the additional fine structure of the D_2 line of ^{85}Rb is represented. The distance D between the two wave packets gives access to the group velocity of the elementary excitations in the transverse plane. The output plane is imaged on a CMOS camera. (Inset, top left) Background-subtracted image obtained for $\theta \simeq 0$ rad and associated integrated envelope profile (blue: original; red dotted: high frequency filtered).

2 Theory

The goal of the phase sensor is to allow for full field retrieval in a propagating superfluid of light experiment. The next section will detail how such a fluid of light can exist in a hot atomic vapor, and its properties. I will first detail the hydrodynamical equations for a fluid of light and show how superfluidity can occur, then I will expose the interest of correlation measurements and finally I will detail the phase retrieval procedure.

2.1 What is a quantum fluid of light ?

The starting point of the system's behavior is the propagation equation of an electric field in a non linear medium, and its quantum version. In our setup, the non-linear medium is a hot Rubidium (^{87}Rb or ^{85}Rb) vapor. This medium presents a third-order non-linearity (Kerr effect), meaning that the standard propagation equation needs to be modified in order to take the non-linearity into account. The following results and derivations are explained in great details in [4].

Paraxial propagation in a Kerr non-linear medium Let $\vec{E}(\vec{r}, t)$ be the electric field of the laser of study. Within the paraxial approximation, it can be decomposed as follows : $\vec{E}(\vec{r}, t) = \mathcal{E}(\vec{r}_\perp, z)e^{i[k(\omega)z - \omega t]}\vec{e}$ where $\mathcal{E}(\vec{r}_\perp, z)$ is the envelope of the field and \vec{e} some arbitrary polarization vector. Then, assuming that the envelope is varying slowly relative to the optical wavelength, the non-linear Schrödinger equation describes the propagation as follows :

$$i\partial_z \mathcal{E}(\vec{r}_\perp, z) = \left[-\frac{1}{2k_0} \vec{\nabla}_\perp^2 - \frac{i\alpha}{2} - \frac{3}{8} \frac{k}{n_0^2} \chi^{(3)}(\omega) |\mathcal{E}(\vec{r}_\perp, z)|^2 \right] \mathcal{E}(\vec{r}_\perp, z). \quad (1)$$

Here k_0 is the wavevector of the field, α is the linear absorption of the medium, n_0 is the regular refractive index of the medium and $\chi^{(3)}(\omega)$ is the third order non-linear electric susceptibility of the medium. The validity of the paraxial treatment has been checked in reference [4]. One can also introduce an external potential (defect) in the cell by optically pumping some region of the cell with another beam closer to the D_2 line of Rb, creating a linear refractive index modulation δn (see fig 1). This adds a term as follows :

$$i\partial_z \mathcal{E}(\vec{r}_\perp, z) = \left[-\frac{1}{2k_0} \vec{\nabla}_\perp^2 - \frac{i\alpha}{2} - k \frac{\delta n(\vec{r}_\perp, z)}{n_0} - \frac{3}{8} \frac{k}{n_0^2} \chi^{(3)}(\omega) |\mathcal{E}(\vec{r}_\perp, z)|^2 \right] \mathcal{E}(\vec{r}_\perp, z). \quad (2)$$

These equations allow to describe "classically" the behavior of the beam inside of the cell but do not allow to describe the quantum effects that take place. To describe these we need to look at the mapping between this non-linear Schrödinger equation and the Gross-Pitaevskii equation.

Gross-Pitaevskii mapping Formally, the third-order non-linearity introduces effective photon-photon interactions that lead to a whole range of effects, the most notable being the superfluid behavior of light inside the cell. Systems of interacting bosons are notoriously described with the Gross-Pitaevskii equation. For example, if $\Psi(\vec{r}, t)$ is the wavefunction of a Bose-Einstein condensate (BEC) within the Hartree-Fock approximation, then $\Psi(\vec{r}, t)$ follows the following equation :

$$i\hbar\partial_t \Psi(\vec{r}, t) = \left[-\frac{\hbar^2}{2m} \vec{\nabla}^2 + V(\vec{r}) + g|\Psi(\vec{r}, t)|^2 \right] \Psi(\vec{r}, t). \quad (3)$$

Here V is an external potential, g is the interaction constant and m the mass of the particles. Neglecting linear absorption ($\alpha \simeq 0$), one can introduce an effective mass, an effective coupling constant and map the propagation to an effective time $\tau = zn_0/c$. Introducing the normalized field envelope $\bar{\mathcal{E}} = \mathcal{E} / \int_S |\mathcal{E}|^2$ where S is the cell cross-section, (1) becomes :

$$i\hbar\partial_\tau \bar{\mathcal{E}}(\vec{r}_\perp, z) = \left[-\frac{\hbar}{2(\hbar k/c)} \vec{\nabla}_\perp^2 - \hbar\omega\delta n(\vec{r}_\perp, z) - \hbar\omega n_2 \mathcal{P}|\bar{\mathcal{E}}(\vec{r}_\perp, z)|^2 \right] \bar{\mathcal{E}}(\vec{r}_\perp, z). \quad (4)$$

One can identify $\bar{m} = \hbar k/c$ the effective mass and the interaction constant $\bar{g} = -\hbar\omega n_2 \mathcal{P}$ with the non-linear refractive index defined as $n_2 = \frac{3}{4c\epsilon_0 n_0^2} \chi^{(3)}$. This mathematically simple analogy is actually conceptually quite subtle as we switch from a 3D+1 geometry to a 2D+1 geometry. We will now display the hydrodynamics properties of the Gross-Pitaevskii equation using a Madelung transform.

Madelung transform and Euler equations One can represent the envelope function of the field $\mathcal{E}(\vec{r}_\perp, z)$ as a density $\rho(\vec{r}_\perp, z)$ and phase $\phi(\vec{r}_\perp, z)$: $\mathcal{E}(\vec{r}_\perp, z) = \sqrt{\rho(\vec{r}_\perp, z)} e^{i\phi(\vec{r}_\perp, z)}$. Injecting this form inside of equation (4) yields :

$$\begin{aligned} \partial_\tau \rho + \vec{\nabla}_\perp \cdot (\rho \vec{v}) + \tilde{\alpha} \rho &= 0 \\ \frac{c}{n_0 k} \partial_\tau \phi + \frac{1}{2} \vec{v}^2 + \frac{c^2}{n_0^2} \left(\frac{n_2}{n_0} \rho + \frac{1}{2k^2} \frac{\vec{\nabla}_\perp^2 \sqrt{\rho}}{\sqrt{\rho}} \right) &= 0 \end{aligned} \quad (5)$$

Here $\vec{v} = \frac{c}{n_0 k} \vec{\nabla}_\perp \phi$ is the speed of the fluid and $\tilde{\alpha} = \alpha/cn_0$ are the losses. This expression is especially interesting because it shows phenomena that have no counterparts in classical hydrodynamics :

- The first equation describes the losses (as opposed to the classical conservation of mass equation) due to linear absorption and thus the Beer-Lambert law.
- The last term of the second equation (in between parenthesis) describes the quantum pressure. This has no classical counterpart and dominates on scales comparable to the healing length (described in the next section).

One finally sees from the expression of the velocity field \vec{v} that to create a flow, one needs to have a gradient of phase, which can be easily achieved using an SLM (spatial light modulator) or the interference pattern between two beams.

Linearization and Bogoliubov transform The Euler equations give great insight into the fluid dynamics of light in a Kerr medium, but these equations have no analytical solutions in general. Furthermore, in order to understand more in details purely quantum effects, one would like a fully quantized equation.

The first natural way to treat these equations is to linearize them. Assuming small perturbations of the density and phase as follows :

$$\begin{aligned} \rho(\vec{r}_\perp, z) &= \rho_0(z) + \delta\rho(\vec{r}_\perp, z) \\ \phi(\vec{r}_\perp, z) &= \phi_0(z) + \delta\phi(\vec{r}_\perp, z) \end{aligned} \quad (6)$$

With $\delta\rho \ll \rho$ and $\delta\phi \ll \phi$. Keeping in mind the $\tau \leftrightarrow z$ mapping, we can then reinject this into (5) and get the linearized equations for $\delta\rho$ and $\delta\phi$ as a function of the propagation distance z . At zeroth order, this simply yields $\rho_0(z) = \rho_0(0)e^{-\alpha z}$ (Beer-Lambert law) and $\partial_z \phi_0 = k_0 n_2 \rho_0$. This last equation describes the Kerr dephasing that the wavefront undergoes. At first order we get :

$$\begin{aligned} \partial_z \delta\rho + \frac{\rho_0}{k} \vec{\nabla}_\perp^2 \delta\phi + \alpha \delta\rho &= 0 \\ \partial_z \delta\phi - k \frac{n_2}{n_0} \delta\rho - \frac{1}{4k} \frac{\vec{\nabla}_\perp^2 \delta\rho}{\rho_0} &= 0 \end{aligned} \quad (7)$$

We can then rewrite $\delta\rho$ and $\delta\phi$ in their second quantized form :

$$\begin{aligned} \delta\rho(\vec{r}_\perp, z) &= \sqrt{\rho_0} \int \frac{d\vec{k}_\perp}{(2\pi)^2} \left[\hat{a}^\dagger(\vec{k}_\perp) f_+(\vec{k}_\perp, z) e^{-i\vec{k}_\perp \cdot \vec{r}_\perp} + h.c \right] \\ \delta\phi(\vec{r}_\perp, z) &= \frac{1}{2i\sqrt{\rho_0}} \int \frac{d\vec{k}_\perp}{(2\pi)^2} \left[\hat{a}^\dagger(\vec{k}_\perp) f_-(\vec{k}_\perp, z) e^{-i\vec{k}_\perp \cdot \vec{r}_\perp} + h.c \right] \end{aligned} \quad (8)$$

Reinjecting these quantized forms into (7) allows us to derive the Bogoliubov-de Gennes matrix equation for the Fourier modes f_+ and f_- :

$$i \frac{\partial}{\partial z} \begin{pmatrix} f_+ \\ f_- \end{pmatrix} = [-i \frac{\alpha}{2} + \mathcal{H}_{\vec{k}_\perp}] \begin{pmatrix} f_+ \\ f_- \end{pmatrix} \text{ where } \mathcal{H}_{\vec{k}_\perp} = \begin{pmatrix} 0 & -\frac{\vec{k}_\perp^2}{2k} \\ -\frac{\vec{k}_\perp^2}{2k} + 2k_0 \Delta n & 0 \end{pmatrix} \quad (9)$$

This matrix describes the mixing of Fourier modes into Bogoliubov modes which are actually **quantized excitations** of the fluid of light. Looking at the spectrum of this matrix allows us to retrieve the spectrum of these excitations (assuming the absorption is small enough for an adiabatic evolution) :

$$\Omega_B(\vec{k}_\perp, z) = i \frac{\alpha}{2} + \sqrt{-\frac{n_2}{n_0} \rho_0(z) \vec{k}_\perp^2 + \frac{\vec{k}_\perp^4}{4k^2}} \quad (10)$$

This dispersion relation has been experimentally measured in [3]. Its most notable feature is its linear behavior at low k_\perp , and quadratic behavior at high k_\perp . This effectively means that low k_\perp excitations have a phonon-like massless behavior whereas the high k_\perp excitations have a massive behavior. The transition occurs at $k_\xi = k \sqrt{\frac{\delta n}{n_0}}$ which is the inverse of the **healing length** ξ of the superfluid. As with atomic BEC's, the healing length is the minimum scale under which the order parameter of the fluid can heal [9], or in more trivial terms, the minimum wavelength of the Bogoliubov excitations. If an excitation has a wavelength under ξ , the excitation energy is too high and locally decondensates the quantum fluid. Once we have this spectrum, we are able to predict the emergence of a superfluid phase through the **Landau criterion for superfluidity** : the system can dissipate through Bogoliubov excitations only if this dissipation is energetically favorable i.e if the following condition is met : assuming we have a static fluid flowing at speed \vec{v} in the transverse plane (following the notations of (5)), nucleating density excitations at \vec{k}_\perp costs $\Omega_B|_{v \neq 0}(\vec{k}_\perp) = \Omega_B|_{v=0}(\vec{k}_\perp) + \vec{k}_\perp \cdot \vec{v}$. This cost must be negative for the nucleation to be energetically favorable. This is the Landau criterion. This criterion is met when $\vec{k}_\perp \cdot \vec{v} < 0$ and $\Omega_B|_{v=0}(\vec{k}_\perp) < |\vec{v}| |\vec{k}_\perp|$ i.e when the excitations are emitted upstream and when the velocity exceeds a certain critical velocity v_c given by :

$$v_c = \min_{\vec{k}_\perp} \left(\frac{\Omega_B|_{v=0}(\vec{k}_\perp)}{|\vec{k}_\perp|} \right) \quad (11)$$

This velocity is referred as the **speed of sound** of the system because it delimits the normal fluid and the superfluid regime of the Bogoliubov dispersion. A remarkable display of the superfluid nature of the fluid of light is depicted in [4] and is reproduced in fig.4.

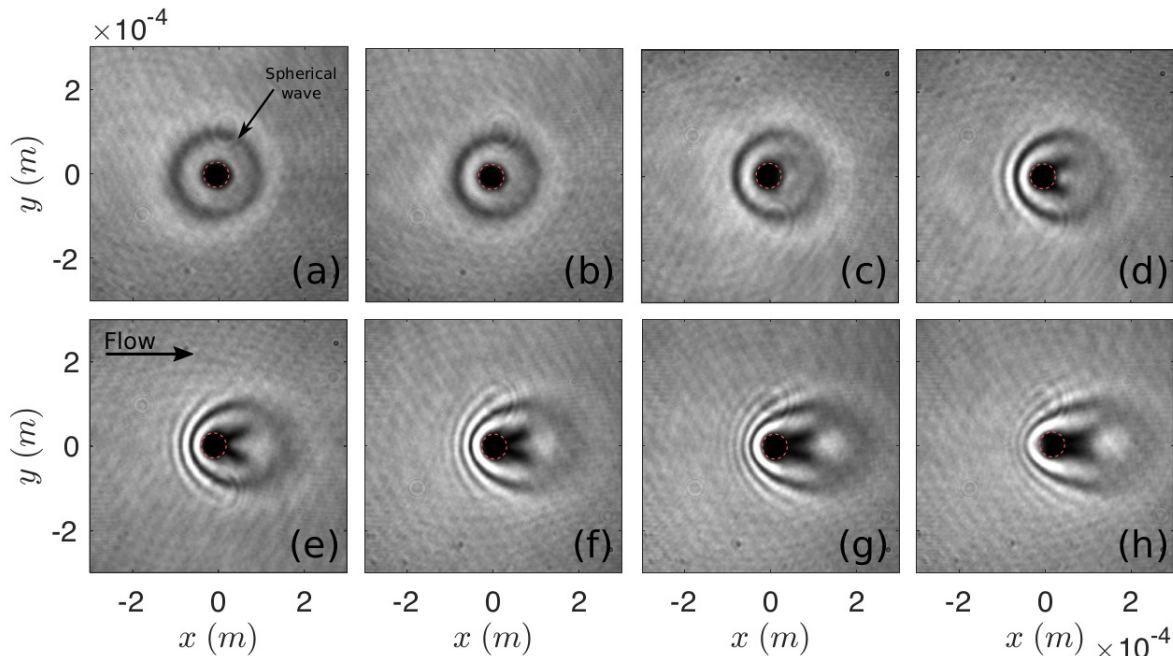


Figure 4: Near-field scattering patterns at low background density ρ_0 . A defect beam generates a negative Gaussian index modulation ($\delta n < 0$), whose width $\omega_{0,d}$, is about $40 \mu\text{m}$. The resulting potential is repulsive explaining why a dark spot is visible at the position where the defect lies (red dotted circle). (a): The photon fluid is at rest ($v = 0$). A spherical wave is created as soon as probe and defect enter the cell and propagate away from the defect. (b)-(h): The photon fluid is flowing rightward. The flow velocity steps up from one image to the next. On figure (d), interference fringes upstream from the obstacle start appearing. Light is scattered backward by the repulsive defect and interferes with the incoming fluid. On (g) and (h), the contrast of the fringes before the obstacle decreases. The kinetic energy of the photon fluid is large compared to the height of the potential and light just go through without being back-scattered. We can finally notice that the spherical wave visible on figure (a) is dragged with the flow and drifts rightward.

As presented in fig.4, when a defect is introduced in the cell using an additional beam, one can see the flow of the fluid of light around the defect, very much like the soundwaves accumulating in front of a fighter jet.

2.2 Correlation measurements

One of the main goals of the paraxial fluid of light platform would be to observe beyond mean field effects, particularly higher-order non-classical correlations induced by the interactions of the Bogoliubov excitations inside of the cell. One way is to study the interferences of Bogoliubov excitations [10]. To that end, full field retrieval would be extremely valuable as it would not only give direct access to the non linear phase accumulated by the light through the cavity, but also to the correlations of the field. From the full field, one can then derive all the moments of the field, including the valuable $g^{(1)}$ and $g^{(2)}$ measurements that give a detailed look of the quantum properties of the system. Furthermore, doing this kind of measurement using full field retrieval would be considerably simpler than other cold atoms techniques that usually involve computing proxima of the actual moments (see [11] for instance).

Recently, quantum fluids of light have been proposed as an experimental platform to explore purely quantum effects from the field of analogue gravity such as quantum vacuum emission from analogue white holes [12] or Hawking radiation and the dynamical Casimir effect around the horizon of an analogue black hole [6]. All of these phenomena display characteristic signatures in terms of density fluctuations i.e intensity fluctuations that are measured through a $g^{(2)}$ intensity correlation measurement. But a

direct $g^{(1)}$ field correlation measurement would give a more detailed view, especially concerning possible phase correlations and their significance, as well as giving access to all possible moments calculations.

2.3 Phase retrieval algorithm

Phase retrieval is a non trivial class of problems, and a very active branch of applied mathematics research. Several methods are available to solve it but in general it is a non convex optimization problem, and it is notoriously hard to solve. One way to solve is is the Gerchberg-Saxton algorithm [13]. However the convergence rate and noise sensitivity of this algorithm is not well controlled. If however one tries to recover the field from several modulated intensity samples i.e ($N \times N$) measurements, it can be shown [14] that full phase retrieval is guaranteed **up to a global phase factor** with an arbitrarily high probability. Furthermore this becomes a convex relaxation of the original problem and can then be solved using existing convex optimization solvers [14]. As presented last year in [1] we use a mix of the two approaches. Following the Gerchberg-Saxton (GS) algorithm, we alternate projections between the source and image planes, but instead of using only one intensity measurement of the field, we propagate several intensity measurements of the **modulated** target field, averaging the result at each iteration.

I will now detail the phase retrieval algorithm. Let $E = Ae^{i\phi}$ be the $N \times N$ target field to recover. K random samples of the field's amplitude \tilde{A}_i ($i \in \llbracket 1, K \rrbracket$) and generated. The modulations are denoted by D_i for intensity masks and Φ_i for phases masks. The intensity modulations are a uniform random distribution of 1 and 0 (binary modulation), and the phase modulations are a uniform random distribution of angles in $[-\pi, \pi]$. The first modulation is kept at unity to initialize the amplitude. Let P_z be the propagation operator that propagates the field over a distance z . The phase retrieval problem is to find E such that $|P_z(ED_i)| = \tilde{A}_i$ (or $|P_z(E\Phi_i)| = \tilde{A}_i$). This is solved using a GS (Gerchberg-Saxton) loop as follows :

- **Initialization** : A non modulated sample $\tilde{A}_1(z)$ is back propagated to the source plane. This yields the initial $\tilde{E}^{(0)}(0)$ guess.
- **Propagation to the image plane** : the initial guess is propagated to the image plane with the modulations $\tilde{E}_i^{(0)}(z) = P_z[\tilde{E}^{(0)}(0)D_i]$. The mean of the root mean square errors of the field estimations $RMS = \frac{1}{N} \langle \|\tilde{E}^{(0)} - E\|_2 \rangle_i$ is computed
- **Amplitude constraint** : Impose the amplitude of the samples to be the measured samples $\tilde{E}_i^{(0)}(z) \leftarrow \tilde{A}_i e^{i[\arg(\tilde{E}_i^{(0)}(z))]}$
- **Back-propagation to the source plane** : Back-propagate the fields to the source plane, taking in to account the modulation, and update the guesses $\tilde{E}_i^{(1)}(0) \leftarrow P_{-z}[\tilde{E}_i^{(0)}(0)]D_i$ (for the phase modulation $\tilde{E}_i^{(1)}(0) \leftarrow P_{-z}[\tilde{E}_i^{(0)}(0)]\Phi_i^{-1}$)
- **Averaging** : Average the guesses to obtain the first estimation of the field : $\tilde{E}^{(1)}(0) = \frac{1}{K} \sum_{i=1}^K \tilde{E}_i^{(1)}(0)$.

The loop stops when the algorithm has converged i.e when the relative variation of the RMS between two iterations falls below 5.10^{-5} . Note that I have found this threshold experimentally as the convergence of the algorithm usually plateaus in the middle, and thus one needs to define a threshold low enough that the algorithm goes past this plateau, but high enough that the algorithm does not continue to loop once retrieval has occurred With a satisfactory precision. The flow chart of the loop can be found in fig.5.

A thorough mathematical analysis of the problem as presented in [14] allows to put precise bounds on the convergence of the algorithm as well as the accuracy of the phase retrieval. The dependence of the number of modulations required for recovery is **logarithmic** in the number of points. This is very interesting in terms of scaling. For a signal of N points, there exists a constant c such that the number of samples needed K follows $K \geq c \log^4(N)$, for a probability of a successful retrieval equals to $1 - \frac{1}{N}$.

Note that the value of the constant c is a priori unknown, but for a signal of 128 points, the authors of [14] find that only 6 samples are needed. For 4024x3036 image, this only goes up to 8 as shown in [1]. For intensity modulation schemes, more samples are needed because the intensity modulated samples carry less information about the field : the zeroes of the mask block half of the pixels. This particularity is discussed in the next section 3.

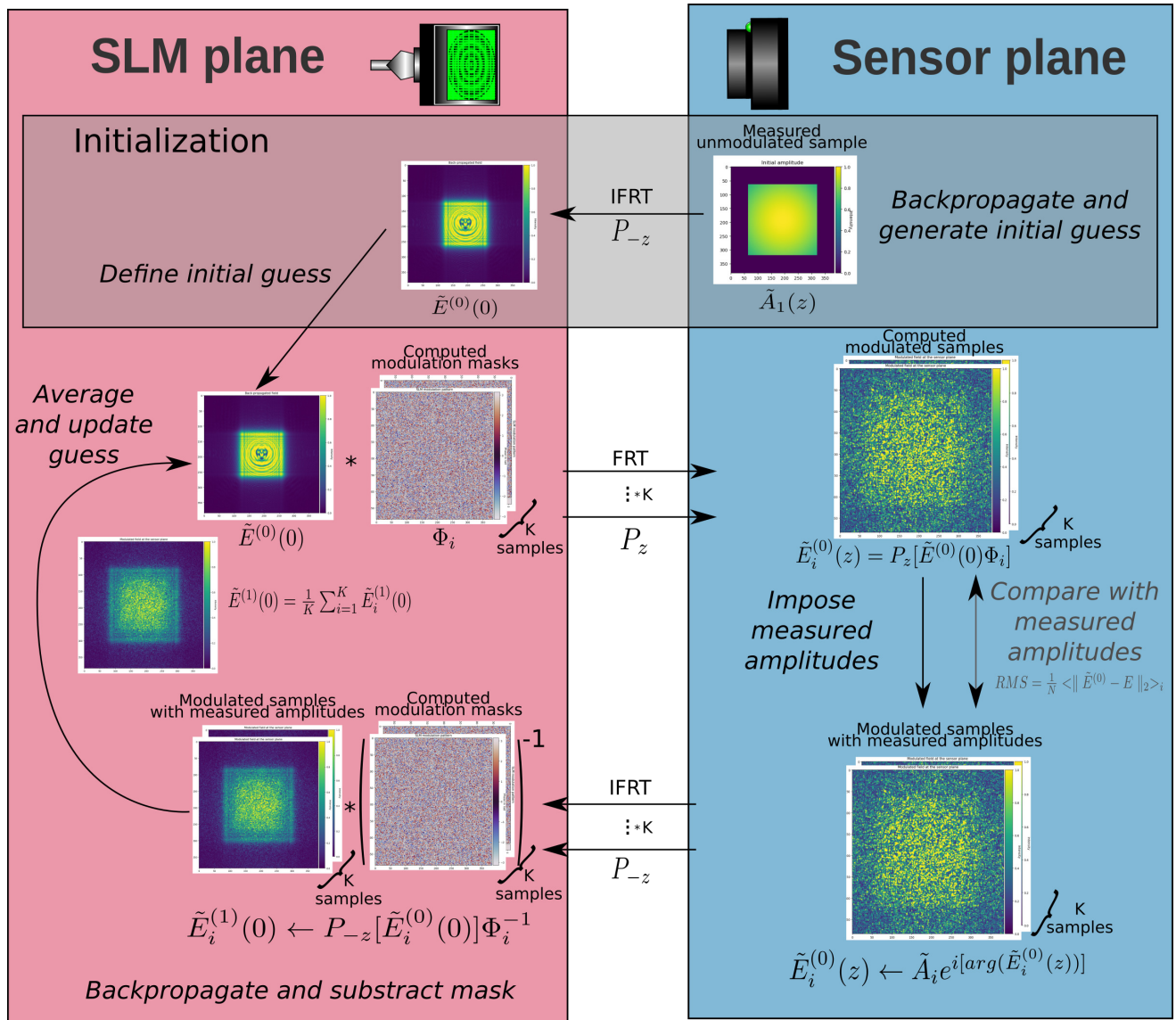


Figure 5: Flow chart of the phase retrieval algorithm : what is the phase associated with the measured unmodulated amplitude $\tilde{A}_1(z)$? FRT and IFRT mean the forward and inverse Fresnel transform i.e the propagation operator over a distance z .

3 Numerical simulations

Given the lack of access to the lab, I had to devise a simulation code in order to develop the software needed for the sensor as well as benchmark its performance. The performance of the code is a critical aspect and is discussed more in detail in subsection 3.2. To generate the modulations of the field realistically, I will simulate the effect of a spatial light modulator (SLM) and a digital micro-mirror device (DMD). An SLM is a liquid crystal screen that allows to apply an arbitrary phase mask to a field, each pixel allowing 256 levels of modulation between 0 and 2π . A DMD is an array of microscopic

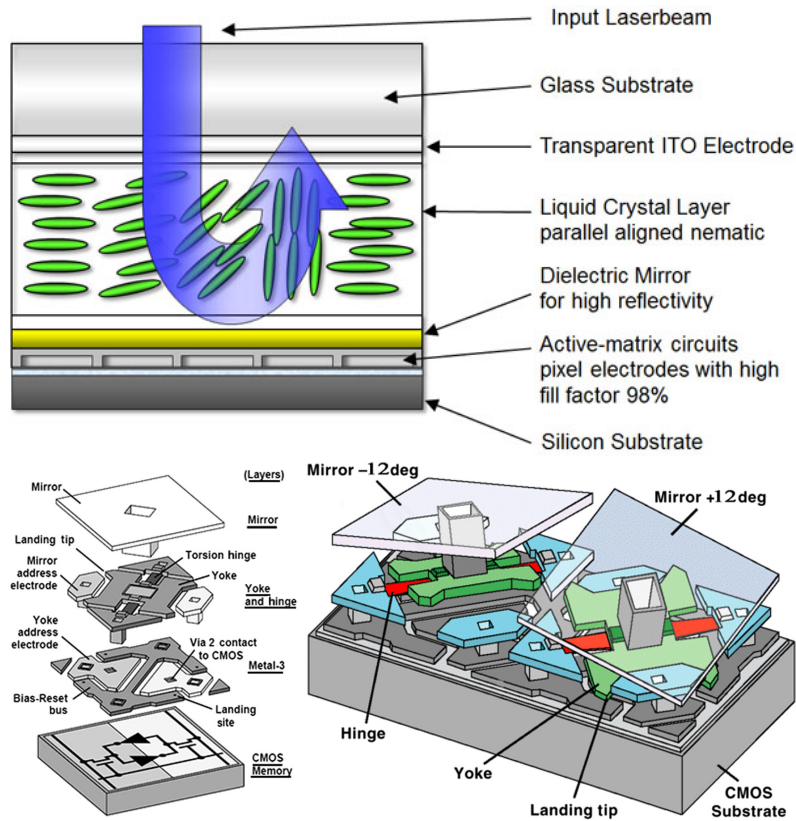


Figure 6: Working principles of an SLM (top) and DMD (bottom). For the SLM, electrodes allow to control the angle of nematic liquid crystals, thus locally modulating the refractive index of the medium. For the DMD, each pixel is simply a mirror placed on a hinge that can be switched from one angle to the other using two electrodes.

mirrors that can be set to two incidence angles : 12 and -12 degrees. This allows to apply an intensity mask to a field by turning "on" or "off" each micro-mirror of the array. The design of these is depicted in fig 6.

3.1 Program structure

The code I've been using for the last month of my internship is divided in two main parts :

- Image production : simulate some signal from which to retrieve the phase map, including the rescaling steps taking into account the various definitions of the camera, SLM or DMD
- Phase retrieval

All of the code is available in the Addendum section, and its latest version can be found on the project's GitHub. Physical parameters and other relevant hard coded parameters are read from a configuration file (see `wish.conf`). The main guideline throughout development was to write a code that would be directly deployable in for the future production code. This meant starting from the sensor plane as this is the main limiting factor in the experimental setup, and anticipating the image processing routines needed for real data acquisition. For this, the help from Yicheng Wu (author of [1]) allowed for massive time savings.

3.1.1 Image production

I start by loading an arbitrary image that will be the signal that we observe on the camera and from which we want to retrieve the phase. I also load some phase pattern of the same size, this phase pattern will at the end be compared to the retrieved wavefront. Then, these images are padded in order to leave some room for the modulated wavefronts. Also as we deal with a lot of Fourier transforms, it is better to introduce protection bands in order to avoid unwanted reflection aliasing (lines 41 to 58 in `WISH_measurement.py`). Then these images are backpropagated to the source plane using the function `u4Tou3` (1.221 of `WISH_1kb.py`). Propagating duties are handled by the `frt` function (1.150/176 of `WISH_1kb.py`). From the field in the source plane, SLM or DMD modulations are generated and applied to the field using `modulate` or `modulate_binary` (1.106/119 of `WISH_1kb.py`). Examples of such modulations can be found in fig 9.

As the different planes of the experiment have different spacings in practice, it is of capital importance that all fields are rescaled relative to one another according to these different spacings to ensure the correct numerical simulation of propagation. More explicitly, the SLM pixel pitch for instance is $12.5 \mu m$, whereas the camera pixel pitch is $5.5 \mu m$. This means that if we want to numerically simulate the effect of the SLM on the wavefront, one needs to resize it so that one pixel of the field has the right physical size when applying the phase mask. As the pixel pitch of the SLM is roughly twice the camera's, this means that the SLM pattern needs to be scaled by a factor of two. As the SLM has an apparent spacing imposed by the Fresnel transform (see equation 12), this means that numerically, the SLM pattern will need to be rescaled by a factor d_{SLM}/d' if d_{SLM} is the SLM pixel pitch, and d' the apparent pitch of the SLM as seen by the camera. If this is not done, the calculation cannot carry on as the SLM has a 1280×1024 definition, whereas the camera has a 2048×2048 . This resizing routine is done by the function `process_SLM` (1.231 of `WISH_1kb.py`).

Finally, modulated fields are propagated to the sensor plane. All of this is done in the `gen_ims` function (1.299 of `WISH_1kb.py`). When propagating, an optional `noise` parameter allows to add a gaussian noise to the field to simulate sensor noise. It can then generate multiple noised copies to then be able to simulate noise averaging. These three steps are presented in fig 7.

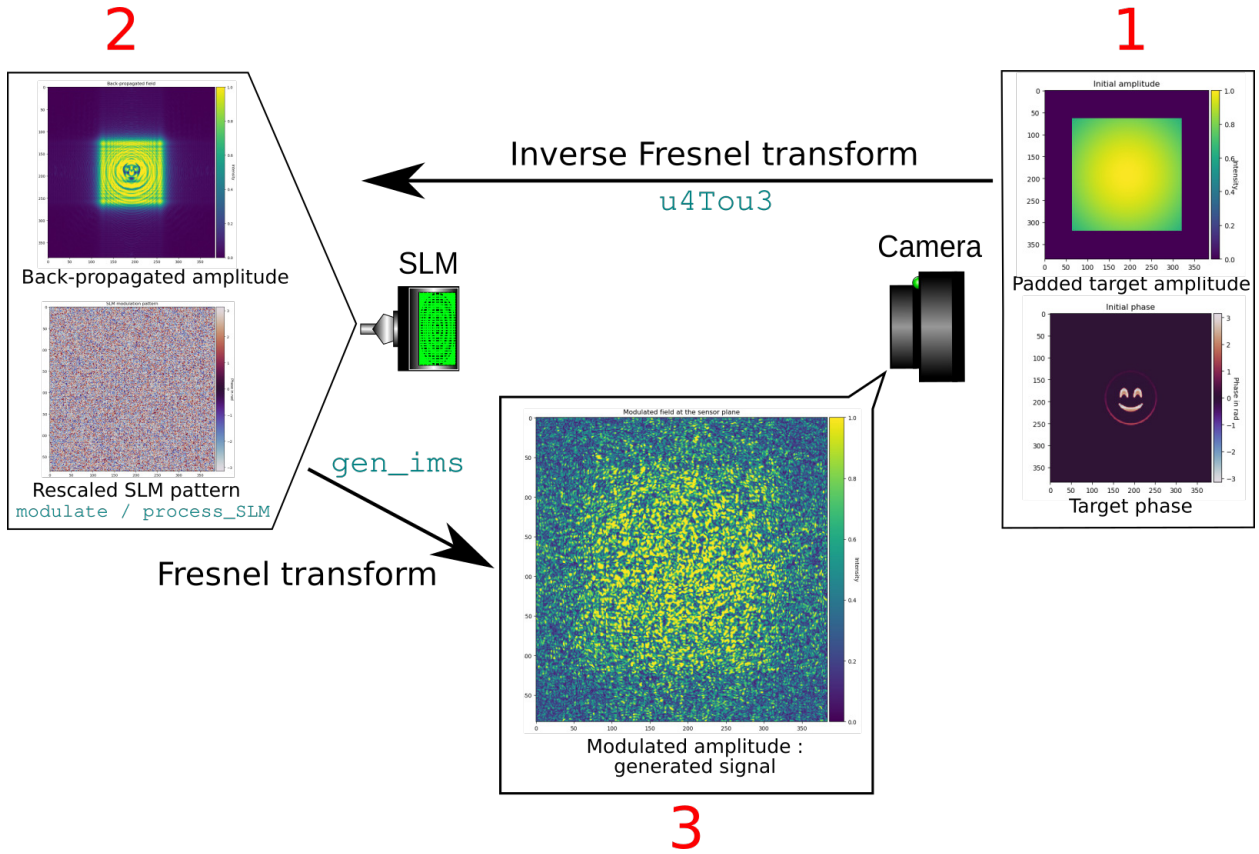


Figure 7: Flowchart of the signal generation. The target field amplitude and phase are first imposed (1) then they are backpropagated to the source plane. At the source plane, the modulation patterns are generated (2) and rescaled according to the relevant physical scales. Finally, the modulation is applied to the field and it is propagated to the sensor plane (3).

3.1.2 Phase retrieval

When the field samples are generated, they are then fed to the main workhorse of the code : `WISHrun` (1.351 of `WISH_1kb.py`). This function is a strict implementation of the algorithm workflow presented in fig 5. It is mainly composed of a double `for` loop : one for the Gerchberg-Saxton (GS) iterations, and inside it, another loop for the samples. Inside the GS loop, propagation is kept to its bare minimum using and optimized propagation function `firt_gpu_s` (1.204 in `WISH_1kb.py`). As we go back and forth between the source and sensor planes, the quadratic and constant phase factors applied in the full Fresnel transform in eq.12 cancel each other out. We are left with almost a bare FFT, only supplemented by two calls to `fftshift` to keep the physical orders of the images. This function is explored more in detail in the next section 3.2 as it has been the subject of a lot of thoughts for the code to run in a reasonable amount of time.

Convergence of the loop is controlled by computing the mean of the normalized root mean square (RMS) deviation between the target amplitudes and current guess, using the built-in `norm` function of Numpy. This RMS is computed only in the signal region, i.e outside of the padding where the intensity is zero. The convergence criterion is when the relative difference of the RMS between two iterations falls below $5 \cdot 10^{-5}$: $\frac{|RMS_{i+1} - RMS_i|}{RMS_i} < 5 \cdot 10^{-5}$. If the convergence criterion is not met in 10000 iterations, the loop stops. Usually, the number of GS iterations is between 40 and 3000 for realistic data sets.

3.2 Need for speed : optimization strategies

A critical aspect of this project is the optimization of the code. For the simulation to run on realistic sets of data, it is crucial that the code is both very fast, but also memory efficient. Effectively, we need to compute at two FFT per sample observation, per GS iteration, as all numerical propagation methods use at least one FFT. In the end, if N_{os} is the number of observations per sample (several images of one modulated samples are taken to try and average noise see section 3.3), N_{mod} the number of modulations and N_{GS} the number of GS iterations, this makes for $N_{os} \times N_{mod} \times N_{GS}$ FFT's. For typical numbers, this makes for $2 \times 16 \times 300 = 9600$ FFT's ! All of this for 2048×2048 pictures or even more depending on the camera ! While this is not computer intensive *per se*, if we want the computation to take less than one minute on a laptop for a "lab compatible" speed, this needs quite a lot of thinking to reach these speeds in Python.

The first step was to depart from external libraries in order to simulate light propagation. At first, I used the Lightpipes library for light propagation with Fresnel transforms. While being very practical and accurate, this library was way too slow and exhaustive for our goals. The order of magnitude of runtime for realistic sets was from 30 minutes to several hours depending on the size of the set. I subsequently coded my own propagation routine using the Fresnel transform presented in [15] :

$$E(x, y, z) = \frac{e^{ikz}}{i\lambda z} e^{i\frac{k}{2z}(x^2+y^2)} \mathcal{F}\{E(x', y', 0) e^{i\frac{k}{2z}(x'^2+y'^2)}\}_{p=\frac{x}{\lambda z}, q=\frac{y}{\lambda z}}. \quad (12)$$

Here E is the scalar electric field, x, y, z are the spatial coordinates and x' and y' are the coordinates in the origin plane. Note that this expression is very convenient for numerical calculations because this means that input and output planes (at 0 and at z) can have different spacings, furthermore this expression can be efficiently computed using fast Fourier transforms (FFT) and a (N, N) discretization of the field. To avoid loss of information however, we will always compute this transform such that the two spacings are Fourier conjugated i.e if the spacing in the sensor plane is d , the reciprocal spacing in the source plane will be $d' = \frac{\lambda z}{Nd}$. After implementing eq.12, I could then convert the code to run on a graphics card (GPU), which are notoriously efficient for array computations such as FFT's.

GPU computing Having no experience in GPU programming, I tried to find the simplest interface to allow me to run calculations on my laptop's GPU (Nvidia MX150, 384 CUDA cores, 2 GB video RAM). Having a Nvidia GPU, I had to find an API (application programming interface) that was using a CUDA C backend. As I had a lot of experience using Numpy for scientific computing, CuPy [16] was the most straightforward option. This library is a drop-in replacement for Numpy and also allows direct access to low level CUDA utilities. This was a game changer and brang a $10\times$ speed up for FFT calculations on 2048×2048 images. Moreover, the speedup gets dramatically larger as size increases (up to $\times 210$ for a 800MB array). The main limitation of GPU computing on my machine was its very small memory capacity (compared to the CPU's RAM) : I have 16GB of RAM on my laptop vs. only 2GB on my GPU, 700MB of which are used by the graphical interface of my operating system. This forced me to work a lot on memory management.

Memory handling After switching to GPU computing, memory management became very important because of the very limited memory "budget" : at first, I could not run any calculation with realistic sizes because my code was so inefficient. The first step was to hunt down useless copies, and other unnecessary uses of memory. Then I reduced the precision wherever possible. As the camera output is coded with a maximum precision of 10 bits, it is meaningless to carry calculations with a precision over 32 bits (for complex numbers). Due to the limitations of the Numpy/CuPy datatypes, and hardware limitations of my GPU (`float16` computations are not really supported on consumer-grade GPU's), I could not go below the `float32` / `complex64` precision. Still, this makes for a factor of two in memory.

Finally, in order to get the best speed, there is a tradeoff between memory economy on the GPU, and memory tranfer times. With CuPy, the data needs to be transfered in the GPU's memory prior

to calculation. This means that it is possible to precisely load only what is needed in the GPU in order to spare memory, but then transfer times penalize execution speed. If on the opposite side, all calculations are ran in a vectorized fashion, meaning by directly feeding a big array with all the samples to the GPU, speed is a lot better, but image size is more limited. Practically, in my code, fields are stored as three dimensional arrays of shape (N, N, N_{im}) where N is the image size, and N_{im} is the total image number ($N_{mod} \times N_{os}$). I can either load this array inside the GPU prior to the GS loop and do all the calculations on the GPU directly, or load individually each batch of N_{os} images inside the GS loop. The first strategy is 35% faster than the second for same size arrays, but the second allows for substantially larger arrays (images up to 2400×2400) or more samples, versus 2048×2048 for the first implementation.

Numba and Cython Python is a flexible and expressive language, however it is not well known for its performance (even though it can be very fast when used properly). This is because Python is a high-level interpreted language and its flexibility actually slows it down drastically. Python spends a lot of time figuring out what the user wants to do. When running a Python code, the code is first compiled in to byte code, then fed to the interpreter that will in term convert it to machine code and actually run it. Upon compilation, one of the most important tasks of the compiler is **type inference** i.e figuring out what types (`float`, `int` etc ...) the variables and various objects should be, allocating memory etc ... After having optimized all functions in terms of algorithmic, this is where we want to try and save some time. There are several ways to speed up this compilation process, but I will only present the two main ones : Numba [17] and Cython [18].

The first way to gain some time on the compilation is to pre-compile some functions that will be heavily used. This can be done with Numba. Numba is a just-in-time compiler, meaning that when running the code, it will compile the properly decorated functions, and store the resulting LLVM (low level virtual machine) code in a cache for further use. This LLVM code is actually the last step before machine code so when the functions run again, it will directly access the cached LLVM code and run drastically faster.

Using Numba is particularly convenient because one only needs to decorate the functions we want to compile just in time ("jit") using the `@jit` command. It can also be used to vectorize functions, and parallelize them. However it is limited in the sense that calls to external libraries are somewhat impossible outside of a few compatible libraries (Numpy and Scipy most notably). Furthermore, one needs to be quite cautious of the way we write functions. Speed up is not automatic and if things are not done properly, one can quite easily end up with a much slower function that what we started with.

Another major way to improve execution speed of Python is to use Cython. Cython allows to use C typing and functions, and compile whole Python scripts or libraries (with their dependences). Actually, almost all Python libraries are compiled using Cython upon installation. Starting from a python script, it is then possible to statically type all of the script by writing a `.pyx` extension that specifies all types and function signatures, very much like a C `.h` header file. Cython also allows to import directly C or C++ modules inside a Python code. This is especially efficient on "light" code where the code in itself does not do heavy computation, where the interpreter overhead is big. Knowing this, I wrote the `.pyx` extension for my `WISH_sensor` class, and then compiled it. Unfortunately, speed up was marginal at best. There are several reasons for this. The bulk of the work of my code is done by either Numpy or CuPy which are two already heavily optimized libraries. The other reason is that CuPy has no official Cython interface, this means that I could not properly type all of the CuPy arrays, nor write custom optimized functions directly using low-level C/Cython code from Cupy, in term greatly hindering the efficiency of the Cythonization.

As a conclusion, as of now, my code is running the fastest it can. It could only run faster if I optimize the `WISHrun` function by rewriting it in CUDA C. I chose not to pursue as it would be a significant step in terms of development time and technicality. As an order of magnitude, the runtime is now around several seconds to 10 minutes depending on the dataset size. For a 300×400 array, phase

retrieval simulation takes 0.2 second with intensity modulations. Compared to the several hours of the first code, this is quite satisfactory. On the hardware side, I did some testing of the code on some more powerful GPU (2018 Nvidia Quadro P2000, 1024 CUDA cores, 5 GB GDDR5) from École Polytechnique computers and I did get a $\times 3$ to $\times 4$ speedup depending on the dataset size. So this means that on more recent GPU's, we could potentially get much more speedup as newer Nvidia GPU's have much larger CUDA core counts (more than $3\times$ larger), significantly higher clock speeds(40% higher), and much larger memory buses ($3\times$ larger). Speedups ranging from $\times 8$ to $\times 16$ seem to be a reasonable estimate, as the added memory would allow to fully vectorize the computations. This would bring the runtime to several seconds for full size 2048×2048 calculations, possibly much less for smaller resolutions.

3.3 Performance benchmarks

In this part I will detail the performance of the phase retrieval procedure for various experimental parameters : number of modulation patterns, type of modulation and noise levels. For benchmarking, I will use a gaussian target amplitude, and the phase pattern presented in fig 8. Besides its comical appearance, I chose an easily recognizable phase pattern with sharp edges and high frequency details in order to test both the accuracy and resolution of the phase retrieval.

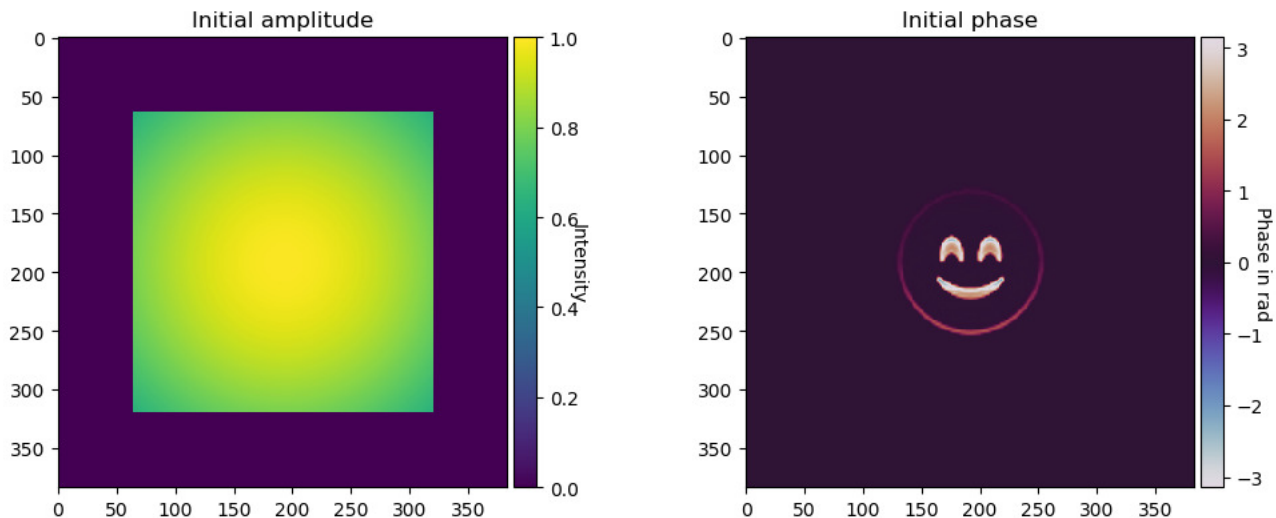


Figure 8: *Initial amplitude (left) and initial phase (right). Both images are 256×256 with an additional padding of 64 pixels.*

The other experimental parameters follow the actual experimental setup (see section 4) : wavelength λ is 634.9 nm, the SLM pixel pitch is $12.5 \mu m$, the DMD pixel pitch is $5.5 \mu m$, the camera pixel pitch is $5.5 \mu m$ and the propagation distance is set to 30 mm. As phase is recovered up to a constant phase factor, accuracy of the phase recovery is estimated by simply computing the minimal normalized *RMS* error when adding a constant phase factor to the recovered phase :

$$RMS_{phase} = \min_{\theta \in [0, 2\pi]} \left[\frac{1}{2\pi N} \left\| \arg(E_{target}) - \arg(e^{i\theta} E_{recovered}) \right\|_2 \right]. \quad (13)$$

Here E_{target} is the target field, $E_{recovered}$ is the recovered field, and N is the size of the region where the *RMS* error is calculated (here 256).

Phase modulation (SLM) Let us start by assessing the effect of the modulation size. Theoretically [14], each pixel should be modulated randomly, however in a physical version of the experiment, the modulation should not diffract the beam so much that it is much larger than the sensor. If this is the

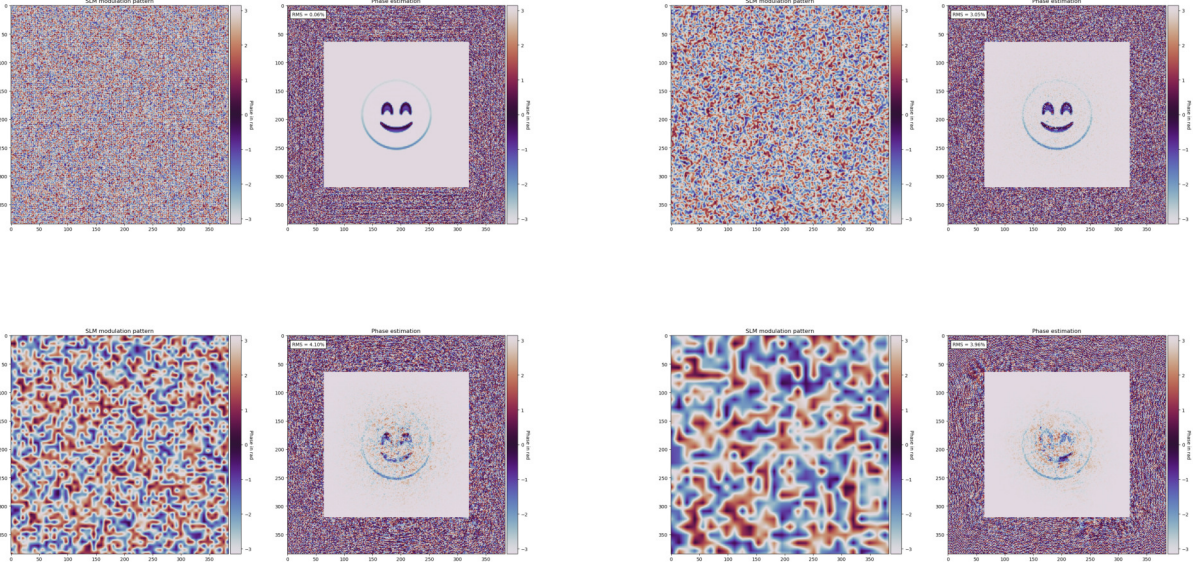


Figure 9: *Impact of the modulation pixel size on phase retrieval. Sample number is 8 and no noise is added. The RMS of the recovered phases from top left to bottom right : 0.06%, 3.05%, 4.10% and 3.96%.*

case, the sensor then acts as a kind of Fourier low-pass filter and prevents the retrieval of fine details. In the same way, if the modulation size is too big, the field will not interfere enough and the retrieval will not be perfect (or not occur at all). For repeatability, the seed of the random number generator is fixed. We compare the results of various pixel sizes in fig 9, setting the modulation number to 8 as recommended in [1].

We see in fig 9 that the quality of the recovered wavefront quickly deteriorates with the increasing pixel size. The RMS in the last 2 picture remains relatively "low" as there is a lot of the target phase pattern that is at $-\pi$, however the loss in quality is very clear. Note that the authors of [1] recommend a pixel size of 10 pixels to avoid excessive diffraction, but their SLM has a pixel size of $5.5 \mu\text{m}$, which is significantly smaller than ours.

We can now look at the influence of the number of modulations on reconstruction accuracy. Taking the SLM modulation size at 1 pixel, we get the following RMS for various sample numbers :

Number of samples K	RMS of the recovered phase
2	0.078 %
8	0.059 %
16	0.049 %

Table 1: *Influence of sample number on recovery for phase modulations*

Augmenting the number of samples improves the convergence, but it also slows it down as the algorithm needs more iterations to converge and the iterations become slower because of the increased number of samples to process. This effect is more pronounced on larger images.

Finally, let us see now the effects of noise on the retrieval. Looking at the specifications of our camera (10 bit Point Grey Grasshopper NIR, 2048×2048 CMOS 1" sensor), we know that the dark noise is 0.02%. We can then realistically look at noise levels from 0.02% to 0.2%. The SLM modulation is kept at its finest size i.e one pixel. Firstly, we test the influence of noise without any noise averaging scheme (taking multiple pictures of the same SLM pattern to average noise). The results can be found

in table 2. We see that the retrieval is quite robust to noise : even at ten times the dark noise of the camera, we still recover a faithful estimate of the target phase map. However the performance of the retrieval is of course reduced. We then redo the same experiment averaging the noise with 10 images for each sample. The results can be found in table 3. This has close to no effect (it even is a bit detrimental), even if we do the average of target amplitudes before the GS loop using 100 images. Also, we note that in the presence of noise, the algorithm stagnates more quickly. Note that in these "realistic" conditions, the performance of the retrieval stays on par with commercial devices such as the Phasics SID4-HR phase camera (following the design presented in [8]), whose rated accuracy on phase recovery is 3.75% .

Noise level	<i>RMS</i> of the recovered phase
0.2%	2.11 %
0.5%	2.81 %
1%	3.67 %
2%	4.12 %

Table 2: *Influence of noise on phase recovery for phase modulations*

Noise level	<i>RMS</i> of the recovered phase
0.2%	2.48 %
0.5%	3.60 %
1%	3.97 %
2%	4.13 %

Table 3: *Influence of noise on phase recovery with a 10 image averaging for phase modulations*

Intensity modulation (DMD) Because of the finer pitch of the DMD, the field gets much more diffracted after reflection. For this reason padding needs to be increased substantially in order to capture a satisfying amount of the field. The following benchmarks will use the same target field as previously, only with a padding of 256 pixels. Let us first study the influence of the number of samples. From an information theory standpoint, as binary intensity modulation give less information about the field than phase modulations, we expect to need more samples to retrieve the phase of the field. We know that on average only half of the pixels are "on", thus to get the information from all the pixels, we need one pattern and its opposite, so we need to multiply by two the number of pattern compared to phase modulations. But then, only half of the pixels have interfered together : "complementary pixels" (from one mask and its opposite) did not interfere together as displayed in fig 10. This is why we need to again multiply by two the number of samples. We subsequently start testing the modulation pixel size with 32 samples. The results of this test are in fig 11.

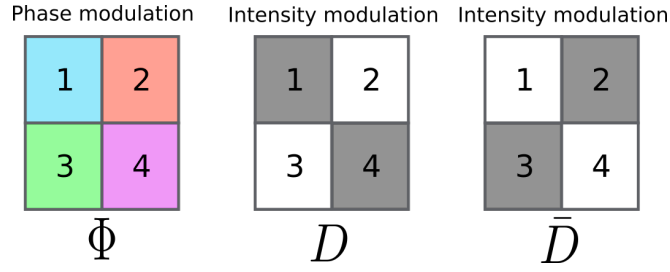


Figure 10: Comparison of the retrieved information between phase and intensity modulations. With the phase modulation, all pixels (1,2,3,4) can interfere together. With intensity modulation, with pattern D only 2 and 3 can interfere, and in \bar{D} only 1 and 4. This means that taking into account D and \bar{D} we have all pixels but interferences only for the couples (2,3) and (1,4) : we miss the couples (1,2) and (3,4).

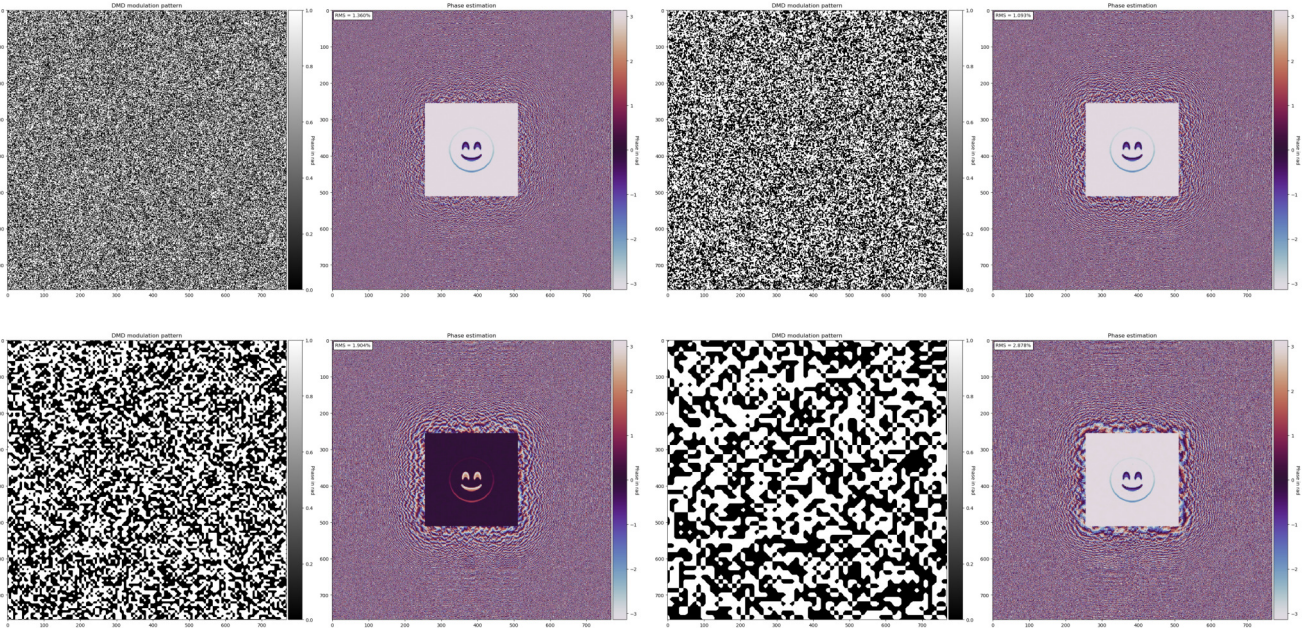


Figure 11: Impact of the modulation pixel size on phase retrieval. Number of samples is 32 and no noise is added. The RMS of the recovered phases from top left to bottom right : 1.36%, 1.09%, 1.90% and 2.88%.

We can see that with the intensity modulation, the optimal size is now at 2 pixels with a padding of 256 pixels. This was expected, as mentioned before, as the field is diffracted a lot more, 2 pixels is the best balance between collection efficiency and sampling of the wavefront. We notice also that the recovery is less sensitive to the change in size of the modulation, certainly due to the increased size of the padding increasing the total size of the images. As before in table 1 we now test the reconstruction accuracy versus the number of samples for a modulation size of 2 pixels : We see that below 8 samples, the recovery breaks down, which was to be expected as it is four times the minimal number theoretically possible, as seen previously with the SLM modulations. Finally, let us assess the robustness of the recovery against noise for 32 samples in tables 5 6.

Then again, the effect of noise averaging is marginal at best, which is quite surprising. Compared to the phase modulations, intensity modulations do seem to be very slightly less sensitive to noise. This can be explained by the higher modulation count.

The conclusion of these benchmarks is that the phase recovery from modulated sample is a very robust and efficient method, having no real bottleneck outside of experimental noise or computational

Number of samples K	RMS of the recovered phase
4	5.78 %
8	3.00 %
16	1.83 %
32	1.10 %
64	1.08 %
128	0.60 %

Table 4: *Influence of the number of samples on recovery for intensity modulations*

Noise level	RMS of the recovered phase
0.2%	1.61 %
0.5%	2.04 %
1%	2.57 %
2%	3.33 %

Table 5: *Influence of noise on the recovery for intensity modulations*

power, achieving sub 1% RMS accuracy for phase recovery.

4 Experimental results

Given the lockdown situation, I could not access the lab at the time I am writing these lines. This means that actually getting an experimental setup to work was challenging to say the least. Hopefully, thanks to the amazing commitment of the lab, the necessary optical components, camera and SLM were sent at my home and I could patch up a working prototype. However due to shipping times and little issues with Thorlabs, I can only present very preliminary results.

Noise level	RMS of the recovered phase
0.2%	1.62 %
0.5%	2.03 %
1%	2.51 %
2%	3.30 %

Table 6: *Influence of noise on the recovery after 10 image averaging for intensity modulations*

4.1 Experimental setup

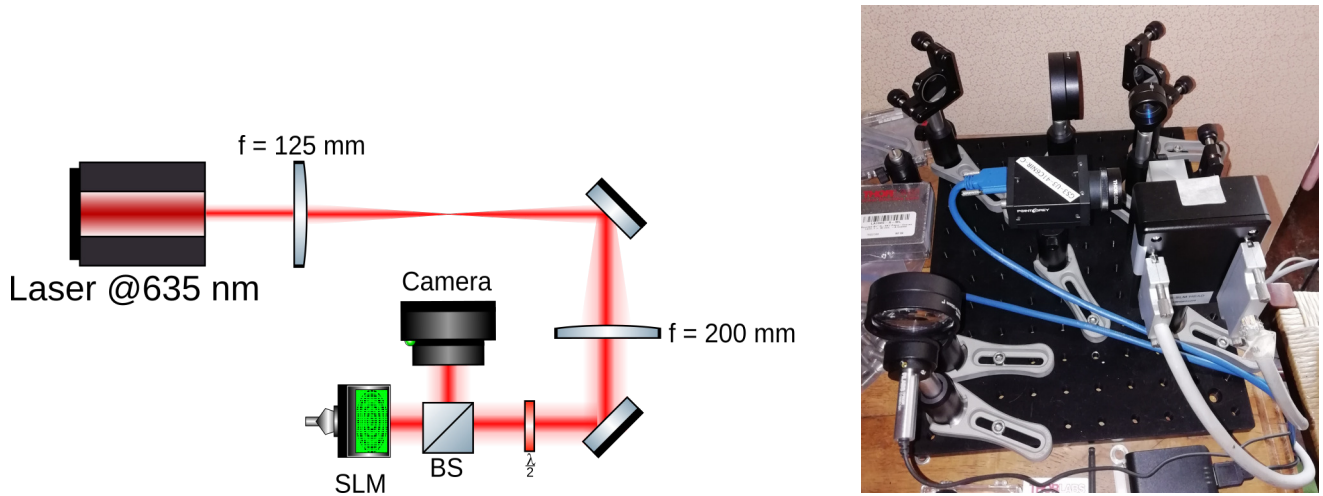


Figure 12: *Left : Experimental setup. The source laser is a Thorlabs CP635R laser diode. It is then expanded by a $\times 1.6$ telescope. Optimal polarization for maximal SLM efficiency is selected using a half-wave plate ($\lambda/2$). The beam is then redirected after reflection to the camera using a non polarizing beam splitter (BS). Right : Picture of the actual setup.*

One of the main appeals of this method for phase retrieval is the simplicity of its experimental setup. As can be seen in 12, the actual measurement setup is composed only of a beam splitter (BS), an SLM and a camera. The test beam is generated using a Thorlabs CP635 red laser diode, then it is expanded using an afocal telescope from two 2 inches plano convex lenses ($f_1 = 125$ mm, $f_2 = 200$ mm). It is then filtered using a half waveplate, and is reflected by the SLM (Hamamatsu LCOS SLM X13138-01, 1280×1024 , $12.5 \mu\text{m}$ pitch). Finally the modulated beam is captured by a CMOS camera (10 bit Point Grey Grasshopper NIR, 2048×2048 CMOS 25.4 mm sensor).

4.2 SLM flatness measurement attempts

The first (and only) measurement I attempted to do was to retrieve the flatness of the SLM. The simplest known dephasing that the beam undergoes is the dephasing due to the SLM surface flatness upon reflection. This information is given by the manufacturer and we can thus check our results against it. Calibration of the SLM head is showed in fig 13. The goal of this measurement is to try and find the phase at the sensor plane, then try to back-propagate it to the SLM plane and compare it with the manufacturer calibration.



Figure 13: *Calibration of the SLM. The flatness of the SLM is here presented in a gray level picture, white is a phase of 0 rad, and black 2π rad.*

The setup is aligned so that the center of the beam coincides with the center of the SLM, and the center of the camera using a Fresnel lensed phase pattern. The images are presented in fig 14. The beam is not perfect and has a high-order Laguerre-Gauss profile, but this is actually beneficial as it helps for the alignment procedure by giving good reference points.

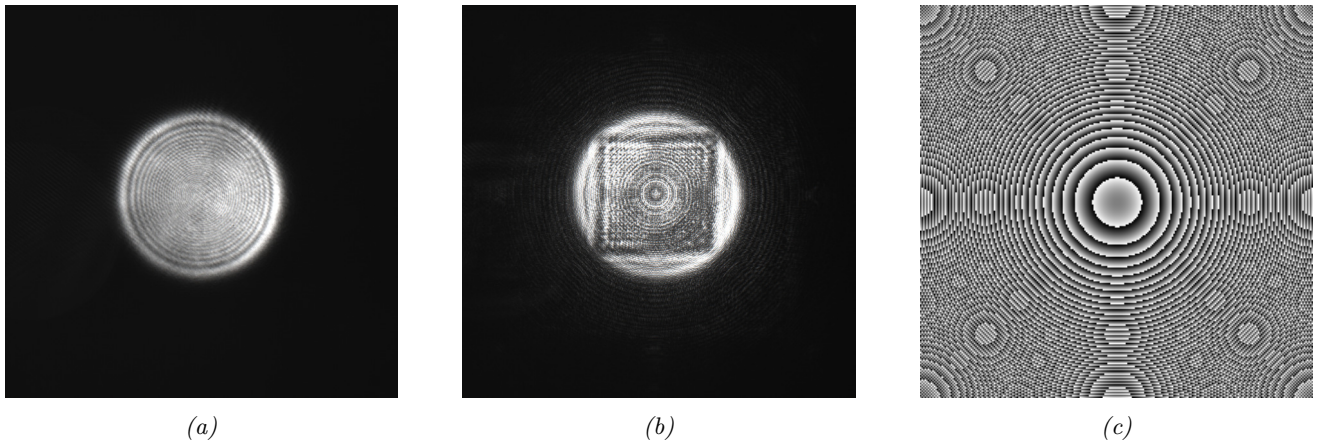


Figure 14: *(a) : Camera view when nothing is displayed on the SLM. (b) : Camera view when the Fresnel pattern is displayed. (c) : Fresnel pattern.*

After this optical alignment procedure that is done by hand, the residual misalignment is taken care of using the Python computer vision library OpenCV. I used the built-in tools of centroid detection to build a simple live centroid detector in order to sight the center of the beam (`alignment.py`), and then translate the image such as the centroid of the beam coincides with the center of the camera. For this I only capture an image and then artificially augment the contrast to facilitate centroid detection. Of course, this introduces artificial margins that are filled with 0, but in any case these areas should not have signal. This numerical alignment procedure is presented in fig 15. This alignment is quite critical as it ensures that when the modulation is applied to the numerical fields, it corresponds to the actual modulation recorded by the camera.

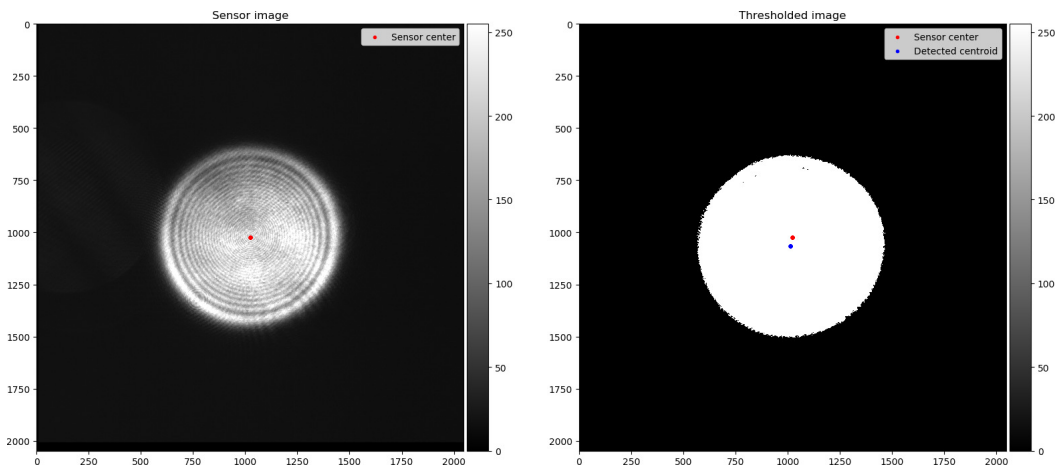


Figure 15: *Centroid detector. The code computes the offset between the red and blue points and can then shift the sensor image so that it is centered.*

The problem with this method is that the centroid detection fails to detect the actual center of the beam. There is a residual error of approximately 5 pixels. This can be seen in fig 15 where the offset between the blue and red points (on the right) is greater than the actual offset that can be seen (on the left). Attempting a measure with 8 samples (the maximum my laptop could handle), one observation per sample gives the following results in fig 16. We see that the amplitude reconstruction is blurred by interference fringes. I suspect they come from the offset between the image and phase field as explained previously. As this image is the mean of the recovery for each sample, the slight misalignment make the different samples interfere. Phase recovery is thus greatly hampered. Looking at the convergence curve, we see however that accuracy on the reconstruction of each sample is quite good as the RMS goes down under 3%. The misalignment might also be due to vibrations during the acquisition as my actual setup is quite shaky due to the fact that I unfortunately do not own an air stabilized optical table at home.

As a conclusion, the sensor does not work for the moment. However, even though the results presented in fig 16 do not show any successful phase retrieval, they confirm that at least amplitude recovery is fonctionnal, thus providing no infirmation of the theoretical simulations. Beam alignment seems to be the critical parameter that remains to be solved. For now, I have put very little effort in to this, and I am confident that I will find a more elegant solution to this alignment problem. Finally, I did not take the time to calibrate the SLM as the algorithm recovers the phase up to a global offset, and as the SLM calibration curve is linear, I thought that this would not be an issue at first. It is quite clear that it will be.

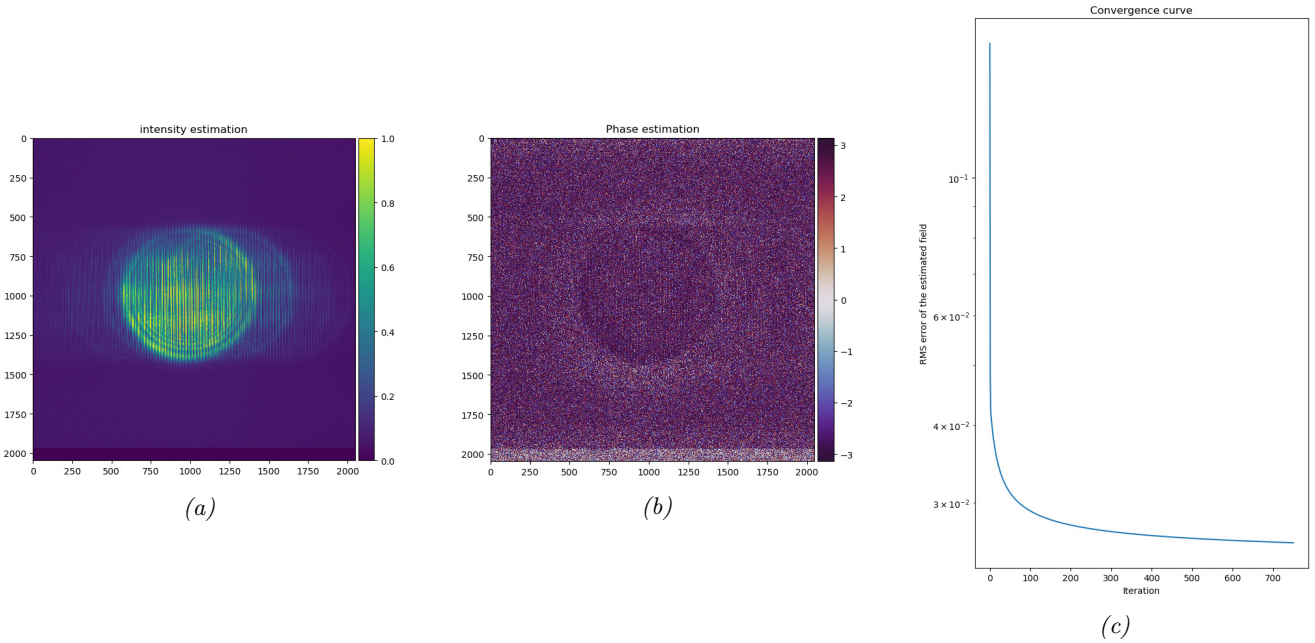


Figure 16: *Phase retrieval measurement attempt with 8 modulation samples. (a) : Reconstructed amplitude. (b) : Reconstructed phase.(c) : Convergence curve (log scale).*

5 Conclusion and outlook

In spite of the very particular circumstances of these first two months of my internship, the workload has been quite intensive and I think a lot a progress was made for this project. I had already a strong background in writing Python for physics and experiment control applications, but this project allowed me to bridge a new step in my coding by discovering GPU programming. If I get the time to do so, I would also like to try and implement this algorithm using a convex solver instead of a Gerchberg-Saxton loop to see if there is any improvement in performance. The material constraints have actually been a very strong catalyser as they forced me to write more efficiently, implementing practical and simple solutions. Furthermore on the experimental side, these conditions are also a good test as the intent of this wavefront sensor on the long run (if its efficiency is validated) would be to be deployed as a cheap and modular solution in the team.

On the more fundamental side, unlocking full phase retrieval would be a big achievement for the main Rubidium experiment, as it would unlock almost direct access to a lot of parameters that were previously hard to derive. Furthermore, it could also be used to set up a retroaction loop, feeding the output field at the input of the cell, thus turning the setup into an actual quantum simulator. This project is also the perfect way for me to set up a lot of the tools and knowledge I will need during my PhD in the team. Besides the purely technical aspect, it allowed me to adapt and integrate in the team in which I will spend the next three years working hard.

References

- [1] Y. Wu, M. K. Sharma, and A. Veeraraghavan, “WISH: wavefront imaging sensor with high resolution,” *Light Sci Appl*, vol. 8, no. 1, p. 44, 2019.
- [2] I. Carusotto and C. Ciuti, “Quantum fluids of light,” *Rev. Mod. Phys.*, vol. 85, no. 1, pp. 299–366, 2013.
- [3] Q. Fontaine, T. Bienaimé, S. Pigeon, E. Giacobino, A. Bramati, and Q. Glorieux, “Observation of the bogoliubov dispersion relation in a fluid of light,” *Physical Review Letters*, vol. 121, no. 18, 2018.
- [4] Q. Fontaine, *Paraxial fluid of light in hot atomic vapor*. PhD thesis, Sorbonne Université, 2019.
- [5] D. Gerace and I. Carusotto, “Analog hawking radiation from an acoustic black hole in a flowing polariton superfluid,” *Phys. Rev. B*, vol. 86, no. 14, p. 144505, 2012.
- [6] I. Carusotto, R. Balbinot, A. Fabbri, and A. Recati, “Density correlations and analog dynamical casimir emission of bogoliubov phonons in modulated atomic bose-einstein condensates,” *Eur. Phys. J. D*, vol. 56, no. 3, pp. 391–404, 2010.
- [7] B. C. Platt and R. Shack, “History and principles of shack-hartmann wavefront sensing,” *J Refract Surg*, vol. 17, no. 5, pp. S573–S577, 2001.
- [8] J.-C. Chanteloup, “Multiple-wave lateral shearing interferometry for wave-front sensing,” *Appl. Opt.*, vol. 44, pp. 1559–1571, Mar 2005.
- [9] L. P. Pitaevskij and S. Stringari, *Bose-Einstein condensation and superfluidity*. No. 164 in International series of monographs on physics, Oxford University Press, reprinted (with corrections) ed., 2016.
- [10] Q. Fontaine, P.-E. Larré, G. Lerario, T. Bienaimé, S. Pigeon, D. Faccio, I. Carusotto, E. Giacobino, A. Bramati, and Q. Glorieux, “Interferences between bogoliubov excitations and their impact on the evidence of superfluidity in a paraxial fluid of light,” *arXiv:2005.14328 [cond-mat.quant-gas]*, 2020.
- [11] J. Armijo, T. Jacqmin, K. V. Kheruntsyan, and I. Bouchoule, “Probing three-body correlations in a quantum gas using the measurement of the third moment of density fluctuations,” *Physical Review Letters*, vol. 105, Nov 2010.
- [12] S. Finazzi and I. Carusotto, “Spontaneous quantum emission from analog white holes in a nonlinear optical medium,” *Physical Review A*, vol. 89, no. 5, p. 053807, 2014.
- [13] R. Gerchberg and W. Saxton, “A practical algorithm for the determination of phase from image and diffraction plane pictures,” *Optik*, vol. 35, pp. 227–246, 1972.
- [14] E. J. Candès, T. Strohmer, and V. Voroninski, “PhaseLift: Exact and stable signal recovery from magnitude measurements via convex programming,” *Communications on Pure and Applied Mathematics*, vol. 66, no. 8, pp. 1241–1274, 2013.
- [15] S. Mehrabkhani and M. Kuester, “Optimization of phase retrieval in the fresnel domain by the modified gerchberg-saxton algorithm,” *arXiv:1711.01176 [physics]*, 2017.
- [16] R. Okuta, Y. Unno, D. Nishino, S. Hido, and C. Loomis, “CuPy: A NumPy-compatible library for NVIDIA GPU calculations,” in *Proceedings of the 31st Conference on Neural Information Processing Systems (NIPS 2017)*, p. 7, 2017.

- [17] S. K. Lam, A. Pitrou, and S. Seibert, “Numba: A llvm-based python jit compiler,” in *Proceedings of the Second Workshop on the LLVM Compiler Infrastructure in HPC*, LLVM ’15, (New York, NY, USA), Association for Computing Machinery, 2015.
- [18] L. Dalcin, R. Bradshaw, K. Smith, C. Citro, S. Behnel, and D. Seljebotn, “Cython: The best of both worlds,” *Computing in Science Engineering*, vol. 13, no. 02, pp. 31–39, 2011.

Addendum : Python codes

Listing 1: *WISH_lkb.py*

```
1 # -*- coding: utf-8 -*-
2 """
3 @author : Tangui ALADJIDI
4 After the Matlab code from Yicheng WU
5 """
6
7
8 import numpy as np
9 import matplotlib.pyplot as plt
10 from PIL import Image
11 from time import time
12 from mpl_toolkits.axes_grid1 import make_axes_locatable
13 import time
14 import sys
15 import configparser
16 import cupy as cp
17 from cupyx.scipy.ndimage import zoom
18
19
20
21 """
22 IMPORTANT NOTE : If the cupy module won't work, check that you have the right
23 → version of CuPy installed for you version
24 of CUDA Toolkit : https://docs-cupy.chainer.org/en/stable/install.html
25 If you are sure of you CuPy install, then it is possible that your nvidia kernel
26 → module froze or that some program
27 bars the access to CuPy. In this case reload your Nvidia module using these commands
28 → (in Unix) :
29     sudo rmmod nvidia_uvm
30     sudo modprobe nvidia_uvm
31 This usually happens after waking up you computer. A CPU version of the code is also
32 → available WISH_lkb_cpu.py
33 """
34
35
36
37
38
39
40
41
42
43
44
45
46
47
48
49
50
51
52
53
54
55
56
57
58
59
60
61
62
63
64
65
66
67
68
69
70
71
72
73
74
75
76
77
78
79
80
81
82
83
84
85
86
87
88
89
90
91
92
93
94
95
96
97
98
99
100
101
102
103
104
105
106
107
108
109
110
111
112
113
114
115
116
117
118
119
120
121
122
123
124
125
126
127
128
129
130
131
132
133
134
135
136
137
138
139
140
141
142
143
144
145
146
147
148
149
150
151
152
153
154
155
156
157
158
159
160
161
162
163
164
165
166
167
168
169
170
171
172
173
174
175
176
177
178
179
180
181
182
183
184
185
186
187
188
189
190
191
192
193
194
195
196
197
198
199
200
201
202
203
204
205
206
207
208
209
210
211
212
213
214
215
216
217
218
219
220
221
222
223
224
225
226
227
228
229
230
231
232
233
234
235
236
237
238
239
240
241
242
243
244
245
246
247
248
249
250
251
252
253
254
255
256
257
258
259
260
261
262
263
264
265
266
267
268
269
270
271
272
273
274
275
276
277
278
279
280
281
282
283
284
285
286
287
288
289
290
291
292
293
294
295
296
297
298
299
300
301
302
303
304
305
306
307
308
309
310
311
312
313
314
315
316
317
318
319
320
321
322
323
324
325
326
327
328
329
330
331
332
333
334
335
336
337
338
339
340
341
342
343
344
345
346
347
348
349
350
351
352
353
354
355
356
357
358
359
360
361
362
363
364
365
366
367
368
369
370
371
372
373
374
375
376
377
378
379
380
381
382
383
384
385
386
387
388
389
390
391
392
393
394
395
396
397
398
399
400
401
402
403
404
405
406
407
408
409
410
411
412
413
414
415
416
417
418
419
420
421
422
423
424
425
426
427
428
429
430
431
432
433
434
435
436
437
438
439
440
441
442
443
444
445
446
447
448
449
450
451
452
453
454
455
456
457
458
459
460
461
462
463
464
465
466
467
468
469
470
471
472
473
474
475
476
477
478
479
480
481
482
483
484
485
486
487
488
489
490
491
492
493
494
495
496
497
498
499
500
501
502
503
504
505
506
507
508
509
510
511
512
513
514
515
516
517
518
519
520
521
522
523
524
525
526
527
528
529
530
531
532
533
534
535
536
537
538
539
540
541
542
543
544
545
546
547
548
549
550
551
552
553
554
555
556
557
558
559
560
561
562
563
564
565
566
567
568
569
570
571
572
573
574
575
576
577
578
579
580
581
582
583
584
585
586
587
588
589
590
591
592
593
594
595
596
597
598
599
600
601
602
603
604
605
606
607
608
609
610
611
612
613
614
615
616
617
618
619
620
621
622
623
624
625
626
627
628
629
630
631
632
633
634
635
636
637
638
639
640
641
642
643
644
645
646
647
648
649
650
651
652
653
654
655
656
657
658
659
660
661
662
663
664
665
666
667
668
669
670
671
672
673
674
675
676
677
678
679
680
681
682
683
684
685
686
687
688
689
690
691
692
693
694
695
696
697
698
699
700
701
702
703
704
705
706
707
708
709
710
711
712
713
714
715
716
717
718
719
720
721
722
723
724
725
726
727
728
729
730
731
732
733
734
735
736
737
738
739
740
741
742
743
744
745
746
747
748
749
750
751
752
753
754
755
756
757
758
759
760
761
762
763
764
765
766
767
768
769
770
771
772
773
774
775
776
777
778
779
780
781
782
783
784
785
786
787
788
789
790
791
792
793
794
795
796
797
798
799
800
801
802
803
804
805
806
807
808
809
810
811
812
813
814
815
816
817
818
819
820
821
822
823
824
825
826
827
828
829
830
831
832
833
834
835
836
837
838
839
840
841
842
843
844
845
846
847
848
849
850
851
852
853
854
855
856
857
858
859
860
861
862
863
864
865
866
867
868
869
870
871
872
873
874
875
876
877
878
879
880
881
882
883
884
885
886
887
888
889
890
891
892
893
894
895
896
897
898
899
900
901
902
903
904
905
906
907
908
909
910
911
912
913
914
915
916
917
918
919
920
921
922
923
924
925
926
927
928
929
930
931
932
933
934
935
936
937
938
939
940
941
942
943
944
945
946
947
948
949
950
951
952
953
954
955
956
957
958
959
960
961
962
963
964
965
966
967
968
969
970
971
972
973
974
975
976
977
978
979
980
981
982
983
984
985
986
987
988
989
990
991
992
993
994
995
996
997
998
999
1000
1001
1002
1003
1004
1005
1006
1007
1008
1009
1010
1011
1012
1013
1014
1015
1016
1017
1018
1019
1020
1021
1022
1023
1024
1025
1026
1027
1028
1029
1030
1031
1032
1033
1034
1035
1036
1037
1038
1039
1040
1041
1042
1043
1044
1045
1046
1047
1048
1049
1050
1051
1052
1053
1054
1055
1056
1057
1058
1059
1060
1061
1062
1063
1064
1065
1066
1067
1068
1069
1070
1071
1072
1073
1074
1075
1076
1077
1078
1079
1080
1081
1082
1083
1084
1085
1086
1087
1088
1089
1090
1091
1092
1093
1094
1095
1096
1097
1098
1099
1100
1101
1102
1103
1104
1105
1106
1107
1108
1109
1110
1111
1112
1113
1114
1115
1116
1117
1118
1119
1120
1121
1122
1123
1124
1125
1126
1127
1128
1129
1130
1131
1132
1133
1134
1135
1136
1137
1138
1139
1140
1141
1142
1143
1144
1145
1146
1147
1148
1149
1150
1151
1152
1153
1154
1155
1156
1157
1158
1159
1160
1161
1162
1163
1164
1165
1166
1167
1168
1169
1170
1171
1172
1173
1174
1175
1176
1177
1178
1179
1180
1181
1182
1183
1184
1185
1186
1187
1188
1189
1190
1191
1192
1193
1194
1195
1196
1197
1198
1199
1200
1201
1202
1203
1204
1205
1206
1207
1208
1209
1210
1211
1212
1213
1214
1215
1216
1217
1218
1219
1220
1221
1222
1223
1224
1225
1226
1227
1228
1229
1230
1231
1232
1233
1234
1235
1236
1237
1238
1239
1240
1241
1242
1243
1244
1245
1246
1247
1248
1249
1250
1251
1252
1253
1254
1255
1256
1257
1258
1259
1260
1261
1262
1263
1264
1265
1266
1267
1268
1269
1270
1271
1272
1273
1274
1275
1276
1277
1278
1279
1280
1281
1282
1283
1284
1285
1286
1287
1288
1289
1290
1291
1292
1293
1294
1295
1296
1297
1298
1299
1300
1301
1302
1303
1304
1305
1306
1307
1308
1309
1310
1311
1312
1313
1314
1315
1316
1317
1318
1319
1320
1321
1322
1323
1324
1325
1326
1327
1328
1329
1330
1331
1332
1333
1334
1335
1336
1337
1338
1339
1340
1341
1342
1343
1344
1345
1346
1347
1348
1349
1350
1351
1352
1353
1354
1355
1356
1357
1358
1359
1360
1361
1362
1363
1364
1365
1366
1367
1368
1369
1370
1371
1372
1373
1374
1375
1376
1377
1378
1379
1380
1381
1382
1383
1384
1385
1386
1387
1388
1389
1390
1391
1392
1393
1394
1395
1396
1397
1398
1399
1400
1401
1402
1403
1404
1405
1406
1407
1408
1409
1410
1411
1412
1413
1414
1415
1416
1417
1418
1419
1420
1421
1422
1423
1424
1425
1426
1427
1428
1429
1430
1431
1432
1433
1434
1435
1436
1437
1438
1439
1440
1441
1442
1443
1444
1445
1446
1447
1448
1449
1450
1451
1452
1453
1454
1455
1456
1457
1458
1459
1460
1461
1462
1463
1464
1465
1466
1467
1468
1469
1470
1471
1472
1473
1474
1475
1476
1477
1478
1479
1480
1481
1482
1483
1484
1485
1486
1487
1488
1489
1490
1491
1492
1493
1494
1495
1496
1497
1498
1499
1500
1501
1502
1503
1504
1505
1506
1507
1508
1509
1510
1511
1512
1513
1514
1515
1516
1517
1518
1519
1520
1521
1522
1523
1524
1525
1526
1527
1528
1529
1530
1531
1532
1533
1534
1535
1536
1537
1538
1539
1540
1541
1542
1543
1544
1545
1546
1547
1548
1549
1550
1551
1552
1553
1554
1555
1556
1557
1558
1559
1560
1561
1562
1563
1564
1565
1566
1567
1568
1569
1570
1571
1572
1573
1574
1575
1576
1577
1578
1579
1580
1581
1582
1583
1584
1585
1586
1587
1588
1589
1590
1591
1592
1593
1594
1595
1596
1597
1598
1599
1600
1601
1602
1603
1604
1605
1606
1607
1608
1609
1610
1611
1612
1613
1614
1615
1616
1617
1618
1619
1620
1621
1622
1623
1624
1625
1626
1627
1628
1629
1630
1631
1632
1633
1634
1635
1636
1637
1638
1639
1640
1641
1642
1643
1644
1645
1646
1647
1648
1649
1650
1651
1652
1653
1654
1655
1656
1657
1658
1659
1660
1661
1662
1663
1664
1665
1666
1667
1668
1669
1670
1671
1672
1673
1674
1675
1676
1677
1678
1679
1680
1681
1682
1683
1684
1685
1686
1687
1688
1689
1690
1691
1692
1693
1694
1695
1696
1697
1698
1699
1700
1701
1702
1703
1704
1705
1706
1707
1708
1709
1710
1711
1712
1713
1714
1715
1716
1717
1718
1719
1720
1721
1722
1723
1724
1725
1726
1727
1728
1729
1730
1731
1732
1733
1734
1735
1736
1737
1738
1739
1740
1741
1742
1743
1744
1745
1746
1747
1748
1749
1750
1751
1752
1753
1754
1755
1756
1757
1758
1759
1760
1761
1762
1763
1764
1765
1766
1767
1768
1769
1770
1771
1772
1773
1774
1775
1776
1777
1778
1779
1780
1781
1782
1783
1784
1785
1786
1787
1788
1789
1790
1791
1792
1793
1794
1795
1796
1797
1798
1799
1800
1801
1802
1803
1804
1805
1806
1807
1808
1809
1810
1811
1812
1813
1814
1815
1816
1817
1818
1819
1820
1821
1822
1823
1824
1825
1826
1827
1828
1829
1830
1831
1832
1833
1834
1835
1836
1837
1838
1839
1840
1841
1842
1843
1844
1845
1846
1847
1848
1849
1850
1851
1852
1853
1854
1855
1856
1857
1858
1859
1860
1861
1862
1863
1864
1865
1866
1867
1868
1869
1870
1871
1872
1873
1874
1875
1876
1877
1878
1879
1880
1881
1882
1883
1884
1885
1886
1887
1888
1889
1890
1891
1892
1893
1894
1895
1896
1897
1898
1899
1900
1901
1902
1903
1904
1905
1906
1907
1908
1909
1910
1911
1912
1913
1914
1915
1916
1917
1918
1919
1920
1921
1922
1923
1924
1925
1926
1927
1928
1929
1930
1931
1932
1933
1934
1935
1936
1937
1938
1939
1940
1941
1942
1943
1944
1945
1946
1947
1948
1949
1950
1951
1952
1953
1954
1955
1956
1957
1958
1959
1960
1961
1962
1963
1964
1965
1966
1967
1968
1969
1970
1971
1972
1973
1974
1975
1976
1977
1978
1979
1980
1981
1982
1983
1984
1985
1986
1987
1988
1989
1990
1991
1992
1993
1994
1995
1996
1997
1998
1999
2000
2001
2002
2003
2004
2005
2006
2007
2008
2009
2010
2011
2012
2013
2014
2015
2016
2017
2018
2019
2020
2021
2022
2023
2024
2025
2026
2027
2028
2029
2030
2031
2032
2033
2034
2035
2036
2037
2038
2039
2040
2041
2042
2043
2044
2045
2046
2047
2048
2049
2050
2051
2052
2053
2054
2055
2056
2057
2058
2059
2060
2061
2062
2063
2064
2065
2066
2067
2068
2069
2070
2071
2072
2073
2074
2075
2076
2077
2078
2079
2080
2081
2082
2083
2084
2085
2086
2087
2088
2089
2090
2091
2092
2093
2094
2095
2096
2097
2098
2099
2100
2101
2102
2103
2104
2105
2106
2107
2108
2109
2110
2111
2112
2113
2114
2115
2116
2117
2118
2119
2120
2121
2122
2123
2124
2125
2126
2127
2128
2129
2130
2131
2132
2133
2134
2135
2136
2137
2138
2139
2140
2141
2142
2143
2144
2145
2146
2147
2148
2149
2150
2151
2152
2153
2154
2155
2156
2157
2158
2159
2160
2161
2162
2163
2164
2165
2166
2167
2168
2169
2170
2171
2172
2173
2174
2175
2176
2177
2178
2179
2180
2181
2182
2183
2184
2185
2186
2187
2188
2189
2190
2191
2192
2193
2194
2195
2196
2197
2198
2199
2200
2201
2202
2203
2204
2205
2206
2207
2208
2209
2210
2211
2212
2213
2214
2215
2216
2217
2218
2219
2220
2221
2222
2223
2224
2225
2226
2227
2228
2229
2230
2231
2232
2233
2234
2235
2236
2237
2238
2239
2240
2241
2242
2243
2244
2245
2246
2247
2248
2249
2250
2251
2252
2253
2254
2255
2256
2257
2258
2259
2260
2261
2262
2263
2264
2265
2266
2267
2268
2269
2270
2271
2272
2273
2274
2275
2276
2277
2278
2279
2280
2281
2282
2283
2284
2285
2286
2287
2288
2289
2290
2291
2292
2293
2294
2295
2296
2297
2298
2299
2300
2301
2302
2303
2304
2305
2306
2307
2308
2309
2310
2311
2312
2313
2314
2315
2316
2317
2318
2319
2320
2321
2322
2323
2324
2325
2326
2327
2328
2329
2330
2331
2332
2333
2334
2335
2336
2337
2338
2339
2340
2341
2342
2343
2344
2345
2346
2347
2348
2349
2350
2351
2352
2353
2354
2355
2356
2357
2358
2359
2360
2361
2362
2363
2364
2365
2366
2367
2368
2369
2370
2371
2372
2373
2374
2375
2376
2377
2378
2379
2380
2381
2382
2383
2384
2385
2386
2387
2388
2389
2390
2391
2392
2393
2394
2395
2396
2397
2398
2399
2400
2401
2402
2403
2404
2405
2406
2407
2408
2409
2410
2411
2412
2413
2414
2415
2416
2417
2418
2419
2420
2421
2422
2423
2424
2425
2426
2427
2428
2429
2430
2431
2432
2433
2434
2435
2436
2437
2438
2439
2440
2441
2442
2443
2444
2445
2446
2447
2448
2449
2450
2451
2452
2453
2454
2455
2456
2457
2458
2459
2460
2461
2462
2463
2464
2465
2466
2467
2468
2469
2470
2471
2472
2473
2474
2475
2476
2477
2478
2479
2480
2481
2482
2483
2484
2485
2486
2487
2488
2489
2490
2491
2492
2493
2494
2495
2496
2497
2498
2499
2500
2501
2502
2503
2504
2505
2506
2507
2508
2509
2510
2511
2512
2513
2514
2515
2516
2517
2518
2519
2520
2521
2522
2523
2524
2525
2526
2527
2528
2529
2530
2531
2532
2533
2534
2535
2536
2537
2538
2539
2540
2541
2542
2543
2544
2545
2546
2547
2548
2549
2550
2551
2552
2553
2554
2555
2556
2557
2558
2559
2560
2561
2562
2563
2564
2565
2566
2567
2568
2569
2570
2571
2572
2573
2574
2575
2576
2577
2578
2579
2580
2581
2582
2583
2584
2585
2586
2587
2588
2589
2590
2591
2592
2593
2594
2595
2596
2597
2598
2599
2600
2601
2602
2603
2604
2605
2606
2607
2608
2609
2610
2611
2612
2613
2614
2615
2616
2617
2618
2619
2620
2621
2622
2623
2624
2625
2626
262
```

```

42     self.N_os = int(conf["params"]["N_os"])    #number of observations per image
         ↪ (to avg noise)
43     self.Nim = self.N_mod * self.N_os
44     self.threshold = float(conf['params']['mask_threshold']) # intensity
         ↪ threshold for the signal region
45     self.noise = float(conf['params']['noise'])
46     def define_mask(self, I: np.ndarray, plot: bool = False):
47         """
48         A function to define the signal region automatically from the provided
↪ intensity and threshold
49         :param I: intensity from which to define a signal region
50         :param threshold: intensities below threshold are discarded
51         :param plot: Plot or not the defined mask
52         :return: mask_sr the defined mask
53         """
54         threshold = self.threshold
55         h, w = I.shape
56         mask_sr = np.zeros((h, w))
57         # detect outermost non zero target intensity point
58         non_zero = np.array(np.where(I > self.threshold))
59         non_zero_offset = np.zeros(non_zero.shape)
60         # offset relative to center
61         non_zero_offset[0] = non_zero[0] - (h / 2) * np.ones(len(non_zero[0]))
62         non_zero_offset[1] = non_zero[1] - (w / 2) * np.ones(len(non_zero[1]))
63         # Determine radii of each non-zero point
64         R_non_zero = np.sqrt(non_zero_offset[0] ** 2 + non_zero_offset[1] ** 2)
65         R_max = np.where(R_non_zero == np.max(abs(R_non_zero)))[0][
66             0]
67         # if there are several equally far points, it takes the
68         # first one
69         i_max, j_max = int(h / 2 + int(abs(non_zero_offset[0][R_max]))), int(
70             w / 2 + int(abs(non_zero_offset[1][R_max])))
71         i_min, j_min = int(h / 2 - int(abs(non_zero_offset[0][R_max]))), int(
72             w / 2 - int(abs(non_zero_offset[1][R_max])))
73         delta_i = int(i_max - i_min)
74         delta_j = int(j_max - j_min)
75         if delta_i > delta_j:
76             mask_sr[i_min:i_max, i_min:i_max] = 1
77             k,l = i_min, i_max
78         else:
79             mask_sr[j_min:j_max, j_min:j_max] = 1
80             k,l = j_min, j_max
81         if plot:
82             fig = plt.figure(0)
83             ax1 = fig.add_subplot(121)
84             ax2 = fig.add_subplot(122)
85             divider1 = make_axes_locatable(ax1)
86             divider2 = make_axes_locatable(ax2)
87             cax1 = divider1.append_axes('right', size='5%', pad=0.05)

```

```

88     cax2 = divider2.append_axes('right', size='5%', pad=0.05)
89     im1=ax1.imshow(I, cmap="viridis")
90     ax1.set_title("Intensity")
91     im2=ax2.imshow(mask_sr, cmap="viridis", vmin=0, vmax=1)
92     ax2.set_title(f"Signal region (Threshold = {threshold})")
93     scat = ax2.scatter(non_zero[0][R_max], non_zero[1][R_max], color='r')
94     scat.set_label('Threshold point')
95     ax2.legend()
96     fig.colorbar(im1, cax=cax1)
97     fig.colorbar(im2, cax=cax2)
98     plt.show()
99     return mask_sr, k,l
100 def crop_center(self, img, cropx, cropy):
101     y, x = img.shape
102     startx = x // 2 - (cropx // 2)
103     starty = y // 2 - (cropy // 2)
104     return img[starty:starty + cropy, startx:startx + cropx]
105 @staticmethod
106 def modulate(shape: tuple, pxsize: int = 10):
107     """
108     A function to randomly modulating a phase map without introducing too much
109     ↪ high frequency noise
110     :param phi: Phase map to be modulated
111     :return: phi_m a modulated phase map to multiply to phi
112     """
113     # generate (N/10)x(N/10) random matrices that will then be upscalled through
114     ↪ interpolation
115     h, w = int(shape[0] / pxsize), int(shape[1] / pxsize)
116     cp.random.seed(1)
117     M = cp.random.rand(h, w) # random matrix between [-1, 1]
118     phi_m = cp.asnumpy(zoom(M, (shape[0]/M.shape[0], shape[1]/M.shape[1])))
119     return phi_m
120 @staticmethod
121 def modulate_binary(shape: tuple, pxsize: int = 10):
122     """
123     A function to randomly modulating a phase map without introducing too much
124     ↪ high frequency noise
125     :param phi: Phase map to be modulated
126     :return: phi_m a modulated phase map to multiply to phi
127     """
128     # generate (N/10)x(N/10) random matrices that will then be upscalled through
129     ↪ interpolation
130     h, w = int(shape[0] / pxsize), int(shape[1] / pxsize)
131     cp.random.seed(1)
132     M = cp.random.choice(cp.asarray([0,1]), (h,w)) # random intensity mask
133     #phi_m = np.kron(M, np.ones((10, 10)))
134     phi_m = cp.asnumpy(zoom(M, shape[0]/M.shape[0]))
135     return phi_m
136 def gaussian_profile(self, I: np.ndarray, sigma: float):

```

```

133     """
134
135     :param I: Intensity to which a gaussian profile is going to be applied
136     :param sigma: Standard deviation of the gaussian profile, in fraction of the
137     ↪ provided intensity size
138     :return: I_gauss : the "gaussianized" intensity
139     """
140
141     h, w = I.shape
142     # define a radial position matrix
143     R = np.zeros((h, w))
144     for i in range(h):
145         for j in range(w):
146             R[i, j] = np.sqrt((h / 2 - i) ** 2 + (w / 2 - j) ** 2)
147     sig = sigma * max(h, w)
148     G = np.exp(-R ** 2 / (2 * sig ** 2))
149     I_gauss = I * G
150     return I_gauss
151
152 @staticmethod
153 def frt(A0: np.ndarray, d1: float, wv: float, z: float):
154     """
155     Implements propagation using Fresnel diffraction
156     :param A0: Field to propagate
157     :param d1: Sampling size of the field A0
158     :param z : Propagation distance in metres
159     :return: A : Propagated field
160     """
161
162     k = 2*np.pi / wv
163     N = A0.shape[0]
164     x = np.linspace(0, N - 1, N) - (N / 2) * np.ones(N)
165     y = np.linspace(0, N - 1, N) - (N / 2) * np.ones(N)
166     d2 = wv * z / (N*d1)
167     X1, Y1 = d1 * np.meshgrid(x, y)[0], d1 * np.meshgrid(x, y)[1]
168     X2, Y2 = d2 * np.meshgrid(x, y)[0], d2 * np.meshgrid(x, y)[1]
169     R1 = np.sqrt(X1 ** 2 + Y1 ** 2)
170     R2 = np.sqrt(X2 ** 2 + Y2 ** 2)
171     D = 1 / (1j*wv*abs(z))
172     Q1 = np.exp(1j*(k/(2*z))*R1**2)
173     Q2 = np.exp(1j*(k/(2*z))*R2**2)
174     if z >=0:
175         A = D * Q2 * (d1**2) * np.fft.fftshift(np.fft.fft2(np.fft.ifftshift(A0 *
176         ↪ Q1, axes=(0,1)), axes=(0,1)), axes=(0,1))
177     elif z<0:
178         A = D * Q2 * ((N*d1) ** 2) *
179         ↪ np.fft.fftshift(np.fft.ifft2(np.fft.ifftshift(A0 * Q1, axes=(0,1)),
180         ↪ axes=(0,1)), axes=(0,1))
181
182     return A
183
184 @staticmethod
185 def frt_gpu(A0: np.ndarray, d1: float, wv: float, z: float):
186     """
187

```

```

178     Implements propagation using Fresnel diffraction. Runs on a GPU using CuPy
→ with a CUDA backend.
179     :param A0: Field to propagate
180     :param d1: Sampling size of the field A0
181     :param wv: Wavelength in m
182     :param z : Propagation distance in metres
183     :return: A : Propagated field
184     """
185     k = 2*np.pi / wv
186     N = A0.shape[0]
187     x = cp.linspace(0, N - 1, N) - (N / 2) * cp.ones(N)
188     y = cp.linspace(0, N - 1, N) - (N / 2) * cp.ones(N)
189     d2 = wv * z / (N*d1)
190     X1, Y1 = d1 * cp.meshgrid(x, y)[0], d1 * cp.meshgrid(x, y)[1]
191     X2, Y2 = d2 * cp.meshgrid(x, y)[0], d2 * cp.meshgrid(x, y)[1]
192     R1 = cp.sqrt(X1 ** 2 + Y1 ** 2)
193     R2 = cp.sqrt(X2 ** 2 + Y2 ** 2)
194     D = 1 / (1j*wv*abs(z))
195     Q1 = cp.exp(1j*(k/(2*z))*R1**2)
196     Q2 = cp.exp(1j*(k/(2*z))*R2**2)
197     if z >=0:
198         A =D * Q2 * (d1**2) * cp.fft.fftshift(cp.fft.fft2(cp.fft.ifftshift(A0 *
→ Q1, axes=(0,1)), axes=(0,1)), axes=(0,1))
199     elif z<0:
200         A =D * Q2 * ((N*d1) ** 2) *
→ cp.fft.fftshift(cp.fft.ifft2(cp.fft.ifftshift(A0 * Q1, axes=(0,1)),
→ axes=(0,1)), axes=(0,1))
201
202     return A
203     @staticmethod
204     def frt_gpu_s(A0: np.ndarray, d1: float, wv: float, z: float, plan = None):
205         """
206         Simplified Fresnel propagation optimized for GPU computing. Runs on a GPU
→ using CuPy with a CUDA backend.
207         :param A0: Field to propagate
208         :param d1: Sampling size of the field A0
209         :param wv: Wavelength in m
210         :param z : Propagation distance in metres
211         :return: A : Propagated field
212         """
213         N = A0.shape[0]
214         D = 1 / (1j*wv*abs(z))
215         if z >=0:
216             A =cp.multiply(D*(d1**2),
→ cp.fft.fftshift(cp.fft.fft2(cp.fft.ifftshift(A0, axes=(0,1)),
→ axes=(0,1)), axes=(0,1))
217         elif z<0:
218             A =cp.multiply(D * ((N*d1) ** 2),
→ cp.fft.fftshift(cp.fft.ifft2(cp.fft.ifftshift(A0, axes=(0,1)),
→ axes=(0,1)), axes=(0,1))

```

```

219     return A
220
221 def u4Tou3(self, u4: np.ndarray, delta4: float, z3: float):
222     """
223     Propagates back a field from the sensor plane to the SLM plane
224     :param u4: Field to propagate back
225     :param delta4: Sampling size of the field u4
226     :param z3: Propagation distance in metres
227     :return: u3 the back propagated field
228     """
229     u3 = self.frt(u4, delta4, self.wavelength, -z3);
230     return u3
231 def process_SLM(self, slm: np.ndarray, N: int, delta3: float, type: str):
232     """
233     Scales the pre submitted SLM plane field (either amplitude of phase) to the
→ right size taking into account the
234 apparent size of the SLM in the sensor field of view.
235 :param slm: Input SLM patterns
236 :param N: Size of the calculation (typically the sensor number of pixels)
237 :param N_batch: Number of images to generate
238 :param delta3: Sampling size of the SLM plane (typically the "apparent"
→ sampling size  $wul*z/N*d\_Sensor$  )
239 :param type : "amp" / "phi" amplitude or phase pattern.
240 :return SLM: Rescaled and properly shaped SLM patterns of size (N,N,N_batch)
241     """
242     delta_SLM = self.d_SLM
243     N_batch = self.N_mod
244     if slm.dtype == 'uint8':
245         slm = slm.astype(float)/256.
246     if slm.ndim == 3:
247         #slm2 = slm[:, 421 : 1501, 0:N_batch] #takes a 1080x1080 square of the
→ SLM
248         slm2 = slm[:, :, 0:N_batch]
249         slm3 = np.empty((N,N,N_batch))
250         #scale SLM slices to the right size
251         for i in range(N_batch):
252             slm1 = cp.asnumpy(zoom(cp.asarray(slm2[:, :, i]), delta_SLM / delta3))
253             if slm1.shape[0]>N or slm1.shape[1]>N:
254                 #print("\rWARNING : The propagation distance must be too small
→ and the field on the sensor is cropped !")
255                 slm3[:, :, i]=self.crop_center(slm1, N, N)
256             else :
257                 slm1 = np.pad(slm1, (int(np.ceil((N - slm1.shape[0]) / 2)), \
258                                 int(np.ceil((N - slm1.shape[1]) / 2))))
259             if slm1.shape[0] > N and slm1.shape[1] > N:
260                 slm3[:, :, i] = slm1[0:N, 0:N]
261             elif slm1.shape[0] > N:
262                 slm3[:, :, i] = slm1[0:N, :]
263             elif slm1.shape[1] > N:

```

```

264         slm3[:, :, i] = slm1[:, 0:N]
265     else :
266         slm3[:, :, i] = slm1
267     if type == "phi":
268         SLM = np.exp(1j * 2 * np.pi * slm3).astype(np.complex64)
269     elif type == "amp":
270         SLM = slm3.astype(np.complex64)
271     else :
272         print("Wrong type specified : type can be 'amp' or 'phi' ! ")
273         raise
274 elif slm.ndim == 2:
275     #slm2 = slm[:, 421:1501]
276     slm2 = slm
277     slm3 = np.empty((N, N))
278     # could replace with my modulate function
279     # scale SLM slices to the right size
280     slm1 = zoom(slm2, delta_SLM / delta3)
281     slm1 = np.pad(slm1, (int(np.ceil((N - slm1.shape[0]) / 2)), \
282                     int(np.ceil((N - slm1.shape[1]) / 2))))
283     if slm1.shape[0] > N and slm1.shape[1] > N:
284         slm3 = slm1[0:N, 0:N]
285     elif slm1.shape[0] > N:
286         slm3 = slm1[0:N, :]
287     elif slm1.shape[1] > N:
288         slm3 = slm1[:, 0:N]
289     else:
290         slm3 = slm1
291     if type == "phi":
292         SLM = np.exp(1j * 2 * np.pi * slm3).astype(np.complex64)
293     elif type == "amp":
294         SLM = slm3.astype(np.complex64)
295     else:
296         print("Wrong type specified : type can be 'amp' or 'phi' ! ")
297         raise
298     return SLM
299 def gen_ims(self, u3: np.ndarray, slm: np.ndarray, z3: float, delta3: float,
300     ↪ noise: float):
301     """
302     ↪ Generates dummy signal in the sensor plane from the pre generated SLM
303     ↪ patterns
304     ↪ :param u3: Initial field in the SLM plane
305     ↪ :param phi0 : Initial phase typically the calibration of the SLM
306     ↪ :param slm : Pre generated slm patterns
307     ↪ :param z3: Propagation distance in metres
308     ↪ :param delta3: "apparent" sampling size of the SLM plane (as seen by the
309     ↪ image plane from z3 m away)
310     ↪ :param Nim: Number of images to generate
311     ↪ :param noise: Intensity of the gaussian noise added to the images
312     ↪ :return ims: Generated signal in the sensor plane of size (N,N,Nim)

```

```

310     """
311     N = u3.shape[0]
312     Nim = self.Nim
313     N_batch = self.N_mod
314     N_os = self.N_os
315     delta_SLM = self.d_SLM
316     L_SLM = delta_SLM * 1080
317     x = np.linspace(0, N - 1, N) - (N / 2) * np.ones(N)
318     y = np.linspace(0, N - 1, N) - (N / 2) * np.ones(N)
319     XX, YY = np.meshgrid(x,y)
320     A_SLM = (np.abs(XX) * delta3 < L_SLM / 2) * (np.abs(YY) * delta3 < L_SLM /
    ↪ 2)
321
322     if slm.dtype=='uint8':
323         slm = slm.astype(float)/256
324     ims = np.zeros((N, N, Nim), dtype=float)
325     for i in range(Nim):
326         sys.stdout.write(f"\rGenerating image {i+1} out of {Nim} ...")
327         sys.stdout.flush()
328         a31 = u3 * A_SLM * slm[:, :, i//N_os]
329         a31 = cp.asarray(a31) #put the field in the GPU
330         a4 = self.frt_gpu(a31, delta3, self.wavelength, z3)
331         w = noise * cp.random.rand(N, N)
332         ya = cp.abs(a4)**2 + w
333         ya[ya<0]=0
334         ims[:, :, i] = cp.asnumpy(ya)
335         del a31, a4, ya
336     return ims
337 def process_ims(self, ims: np.ndarray, N: int):
338     """
339     Converts images to amplitudes and eventually resizes them.
340     :param ims: images to convert
341     :param N: Size of the sensor
342     :return y0 : Processed field of size (N,N, Nim)
343     """
344     if ims.dtype!=float:
345         ims=(ims/256).astype(float)
346     y0 = np.real(np.sqrt(ims)); # change from intensity to magnitude
347     y0 = np.pad(y0, (round((N - y0.shape[0]) / 2), round((N - y0.shape[1]) /
    ↪ 2)))
348     if y0.shape[0] > N:
349         y0=y0[0:N,0:N,:]
350     return y0
351 def WISHrun(self, y0: np.ndarray, SLM: np.ndarray, delta3: float, delta4: float,
    ↪ plot: bool=True):
352     """
353     Runs the WISH algorithm using a Gerchberg Saxton loop for phase retrieval.
354     :param y0: Target modulated amplitudes in the sensor plane
355     :param SLM: SLM modulation patterns

```

```

356         :param delta3: Apparent sampling size of the SLM as seen from the sensor
→ plane
357         :param delta4: Sampling size of the sensor plane
358         :param N_os: Number of observations per image
359         :param N_iter: Maximal number of Gerchberg Saxton iterations
360         :param N_batch: Number of batches (modulations)
361         :param plot: If True, plots the advance of the retrieval every 10 iterations
362         :return u4_est, idx_converge: Estimated field of size (N,N) and the
→ convergence indices to check convergence
363                 speed
364         """
365         wvl = self.wavelength
366         z3 = self.z
367         ## parameters
368         N = y0.shape[0]
369         N_batch = self.N_mod
370         N_os = self.N_os
371         N_iter = self.N_gs
372         u3_batch = cp.zeros((N, N, N_os), dtype=cp.complex64) # store all U3 gpu
373         u4 = cp.zeros((N, N, N_os), dtype=cp.complex64) # gpu
374         y = cp.zeros((N, N, N_os), dtype=cp.complex64) # store all U3 gpu
375         ## initilize a3
376         k = 2 * np.pi / wvl
377         xx = cp.linspace(0, N - 1, N, dtype=cp.float) - (N / 2) * cp.ones(N,
→ dtype=cp.float)
378         yy = cp.linspace(0, N - 1, N, dtype=cp.float) - (N / 2) * cp.ones(N,
→ dtype=cp.float)
379         X, Y = float(delta4) * cp.meshgrid(xx, yy)[0], float(delta4) *
→ cp.meshgrid(xx, yy)[1]
380         R = cp.sqrt(X ** 2 + Y ** 2)
381         Q = cp.exp(1j*(k/(2*z3))*R**2)
382         del xx, yy, X, Y, R
383         SLM = cp.asarray(SLM)
384         y0 = cp.asarray(y0)
385         SLM_batch = SLM[:, :, 0]
386         for ii in range(N_os):
387             y0_batch = y0[:, :, ii]
388             u3_batch[:, :, ii] = self.frt_gpu_s(y0_batch/Q, delta4, self.wavelength,
→ -z3) * cp.conj(SLM_batch) #y0_batch gpu
389         u3 = cp.mean(u3_batch, 2)
390         #i_mask, j_mask = self.define_mask(np.abs(y0[:, :, 0]) ** 2, plot=True)[1:3]
391         ## Recon run : GS loop
392         idx_converge = np.empty(N_iter)
393         for jj in range(N_iter):
394             sys.stdout.flush()
395             u3_collect = cp.zeros(u3.shape, dtype=cp.complex64)
396             idx_converge0 = np.empty(N_batch)
397             for idx_batch in range(N_batch):
398                 # put the correct batch into the GPU

```

```

399     SLM_batch = SLM[:, :, idx_batch]
400     y0_batch = y0[:, :, int(N_os * idx_batch): int(N_os * (idx_batch+1))]
401     for _ in range(N_os):
402         u4[:, :, _] = self.frt_gpu_s(u3 * SLM_batch, delta3,
403             → self.wavelength, z3) # U4 is the field on the sensor
404         y[:, :, _] = y0_batch[:, :, _] * cp.exp(1j * cp.angle(u4[:, :, _]))
405             → #impose the amplitude
406         #[:, :, _] = u4[:, :, _]
407         #y[i_mask:j_mask, i_mask:j_mask, _] =
408             → y0_batch[i_mask:j_mask, i_mask:j_mask, _] \
409             #
410             → cp.exp(1j *
411             → cp.angle(u4[i_mask:j_mask, i_mask:j_mask, _]))
412         u3_batch[:, :, _] = self.frt_gpu_s(y[:, :, _], delta4,
413             → self.wavelength, -z3) * cp.conj(SLM_batch)
414     u3_collect = u3_collect + cp.mean(u3_batch, 2) # collect(add) U3
415             → from each batch
416     # convergence index matrix for each batch
417     idx_converge0[idx_batch] = (1/N)*\
418     cp.linalg.norm((cp.abs(u4)-(1/N**2)*cp.sum(cp.abs(SLM_batch))*
419     y0_batch)*(y0_batch>0)) #eventual mask absorption
420
421     u3 = (u3_collect / N_batch) # average over batches
422     idx_converge[jj] = np.mean(idx_converge0) # sum over batches
423     sys.stdout.write(f"\rGS iteration {jj + 1}")
424     sys.stdout.write(f" (convergence index : {idx_converge[jj]})")
425
426     if jj % 10 == 0 and plot:
427         u4_est = cp.asnumpy(self.frt_gpu_s(u3, delta3, self.wavelength, z3)
428             → * Q)
429         plt.close('all')
430         fig=plt.figure(0)
431         fig.suptitle(f'Iteration {jj}')
432         ax1=fig.add_subplot(121)
433         ax2=fig.add_subplot(122)
434         im=ax1.imshow(np.abs(u4_est), cmap='viridis')
435         ax1.set_title('Amplitude')
436         ax2.imshow(np.angle(u4_est), cmap='viridis')
437         ax2.set_title('Phase')
438
439         fig1=plt.figure(1)
440         ax = fig1.gca()
441         ax.plot(np.arange(0,jj,1), idx_converge[0:jj], marker='o')
442         ax.set_xlabel('Iterations')
443         ax.set_ylabel('Convergence estimator')
444         ax.set_title('Convergence curve')
445         plt.show()
446         time.sleep(2)

```

```

441
442     # exit if the matrix doesn 't change much
443     if jj > 1:
444         if cp.abs(idx_converge[jj] - idx_converge[jj - 1]) /
445             ↪ idx_converge[jj] < 1e-5:
446             #if cp.abs(idx_converge[jj]) < 5e-3:
447             #if idx_converge[jj]>idx_converge[jj-1]:
448                 print('\nConverged. Exit the GS loop ...')
449                 #idx_converge = idx_converge[0:jj]
450                 idx_converge = cp.asnumpy(idx_converge[0:jj])
451                 break
452     u4_est = self.frt_gpu_s(u3, delta3, self.wavelength, z3) * Q #propagate
453     ↪ solution to sensor plane
454     return u3, u4_est, idx_converge

```

Listing 2: *WISH_measurement.py*

```

1  # -*- coding: utf-8 -*-
2  """
3  Created by Tangui Aladjidi at 28/05/2020
4  """
5
6  import numpy as np
7  import matplotlib.pyplot as plt
8  from PIL import Image
9  from time import time
10 from mpl_toolkits.axes_grid1 import make_axes_locatable
11 import time
12 import sys
13 import configparser
14 import cupy as cp
15 from scipy.ndimage import zoom
16 from WISH_lkb import WISH_Sensor
17 import slmpy
18 import cv2
19 import EasyPySpin
20
21 #WISH routine
22 def alignment(frame):
23     frame_blurred = cv2.blur(frame, (12, 12))
24     ret1, thresh = cv2.threshold(frame, 70, 255, 0)
25     thresh_blurred = cv2.blur(thresh, (12, 12))
26     M = cv2.moments(thresh_blurred)
27     cX = int(M["m10"] / M["m00"])
28     cY = int(M["m01"] / M["m00"])
29     T = np.float32([[1, 0, int(frame.shape[1]/2) - cX], [0, 1, int(frame.shape[0]/2)
30     ↪ - cY]])

```

```

30     frame_s = cv2.warpAffine(frame, T, frame.shape)
31     return frame_s
32 def main():
33     #start timer
34     T0 = time.time()
35     #instantiate WISH
36     Sensor = WISH_Sensor("wish_3.conf")
37     wvl = Sensor.wavelength
38     z3 = Sensor.z
39     delta4 = Sensor.d_CAM
40     '''
41     To generate images from scratch
42     #IO = np.array(Image.open('intensities/harambe_512_full.bmp'))[:, :, 0]
43     #IO = IO.astype(float)/256
44     #IO = np.pad(IO.astype(np.float) / 256, (256, 256)) # protection band
45     im = np.array(Image.open('intensities/IO_256_full.bmp'))[:, :, 0]
46     phi0 = np.array(Image.open('phases/smiley_256.bmp'))[:, :, 0]
47     im = cp.asnumpy(zoom(cp.asarray(im), 2))
48     phi0 = cp.asnumpy(zoom(cp.asarray(phi0), 2))
49     u40 = np.pad(im.astype(np.float)/256, (768, 768)) #protection band
50     u40 = Sensor.gaussian_profile(u40, 0.5)
51     phi0 = np.pad(phi0.astype(np.float)/256, (768,768)) #protection band
52     u40 = u40 * (np.exp(1j * phi0 * 2 * np.pi))
53     u40=u40.astype(np.complex64)
54     N = u40.shape[0]
55     delta3 = wvl * z3 / (N * delta4)
56     u30 = Sensor.u4Tou3(u40, delta4, z3)
57     ## forward prop to the sensor plane with SLM modulation
58     print('Generating simulation data images ...')
59     noise = Sensor.noise
60     '''
61     slm = np.zeros((1080, 1920, Sensor.N_mod))
62     slm_type = 'SLM'
63     #Setting up the camera for acquisition
64     Cam = EasyPySpin.VideoCapture(0) #by default camera 0 is the laptop webcam
65
66     N = int(Cam.get(cv2.CAP_PROP_FRAME_WIDTH)*1)
67     delta3 = wvl * z3 / (N * delta4)
68     ims = np.zeros((N,N,Sensor.Nim))
69     if slm_type=='DMD':
70         slm = np.ones((1080, 1920, Sensor.N_mod))
71         slm_display = slmpy.SLMdisplay()
72         slm_display.updateArray(slm[:, :, 0])
73         print(f"Displaying 1 st SLM pattern")
74         for obs in range(Sensor.N_os):
75             ret, frame = Cam.read()
76             frame = alignment(frame)
77             ims[:, :, obs] = zoom(cv2.flip(frame, 0), 0.5)
78         for i in range(1,int(Sensor.N_mod/2)):

```

```

79     slm[:, :, 2 * i] = Sensor.modulate_binary((1080, 1920), pxsize=1)
80     for obs in range(Sensor.N_os):
81         ret, frame = Cam.read()
82         frame = alignment(frame)
83         ims[:, :, 2 * i + obs] = zoom(cv2.flip(frame, 0), 0.5)
84     slm[:, :, 2 * i + 1] = np.ones((1080, 1920)) - slm[:, :, 2 * i]
85     for obs in range(Sensor.N_os):
86         ret, frame = Cam.read()
87         frame = alignment(frame)
88         ims[:, :, 2 * i + 1 + obs] = zoom(cv2.flip(frame, 0), 0.5)
89     elif slm_type=='SLM':
90         slm = np.ones((1024, 1280, Sensor.N_mod))
91         slm_display = slmpy.SLMdisplay()
92         slm_display.updateArray(slm[:, :, 0])
93         print(f"Displaying 1 st SLM pattern")
94         for obs in range(Sensor.N_os):
95             ret, frame = Cam.read()
96             frame = alignment(frame)
97             ims[:, :, obs] = zoom(cv2.flip(frame, 0), 1)
98         for i in range(1, Sensor.N_mod):
99             slm[:, :, i] = Sensor.modulate((1024, 1280), pxsize=1)
100            slm_display.updateArray(slm[:, :, i])
101            for obs in range(Sensor.N_os):
102                ret, frame = Cam.read()
103                frame = alignment(frame)
104                ims[:, :, i + obs] = zoom(cv2.flip(frame, 0), 1)
105            print(f"Displaying {i+1} th SLM pattern")
106            slm_display.close()
107            Cam.release()
108     if slm_type == 'DMD':
109         SLM = Sensor.process_SLM(slm, N, delta3, type="amp")
110         SLM[np.abs(SLM) > 0.5] = 1 + 1j*0
111         SLM[SLM <= 0.5] = 0 + 1j*0
112         #fig = plt.figure(1)
113         #ax1 = fig.add_subplot(121)
114         #ax2 = fig.add_subplot(122)
115         #ax1.imshow(np.abs(SLM[:, :, Sensor.N_os]), vmin=0, vmax=1)
116         #ax2.imshow(np.abs(u30), vmin=0, vmax=1)
117         #plt.show()
118     elif slm_type == 'SLM':
119         SLM = Sensor.process_SLM(slm, N, delta3, type="phi")
120         #fig = plt.figure(1)
121         #ax1 = fig.add_subplot(121)
122         #ax2 = fig.add_subplot(122)
123         #ax1.imshow(np.angle(SLM[:, :, Sensor.N_os]), vmin=-np.pi, vmax = np.pi)
124         #ax2.imshow(np.abs(u30), vmin=0, vmax=1)
125         #plt.show()
126     #ims = Sensor.gen_ims(u30, SLM, z3, delta3, noise)
127

```

```

128     print('\nCaptured images are simulated')
129     #reconstruction
130     #process the captured image : converting to amplitude and padding if needed
131     ims=(ims/255.0).astype(np.float)
132     y0 = Sensor.process_ims(ims, N)
133     plt.imshow(y0[:, :, Sensor.N_os], vmin=0, vmax=1)
134     plt.scatter(N/2, N/2, color='r', marker='.')
135     plt.show()
136     ##Recon initialization
137     T_run_0=time.time()
138     u3_est, u4_est, idx_converge = Sensor.WISHrun(y0, SLM, delta3, delta4,
139     ↪ plot=False)
140     T_run=time.time()-T_run_0
141     #phase_rms = cp.corrcoef(cp.ravel(cp.angle(cp.asarray(u40))),
142     ↪ cp.ravel(cp.angle(u4_est)))[0,1]
143     u3_est = cp.asnumpy(u3_est)
144     u4_est = cp.asnumpy(u4_est)
145     #phase_RMS =(1/N) * np.array(
146     #     [np.linalg.norm((np.angle(u40)-np.angle(np.exp(1j*th)*u4_est))*(np.abs(u40)
147     ↪ > 0)) for th in
148     #     np.linspace(-np.pi, np.pi, 256)])
149     #phase_rms = np.min(phase_RMS)
150     #phase_rms
151     ↪ =(1/N)*np.linalg.norm((np.angle(u30)-np.angle(u3_est))*(np.abs(u30)>0))
152     #print(f"\n Phase RMS is : {phase_rms}")
153     #total time
154     T= time.time()-T0
155     print(f"\n Time spent in the GS loop : {T_run} s")
156     print(f"\n Total time elapsed : {T} s")
157     fig=plt.figure()
158     #ax1 = fig.add_subplot(231)
159     #ax2 = fig.add_subplot(232)
160     #ax3 = fig.add_subplot(233)
161     #ax4 = fig.add_subplot(234)
162     #ax5 = fig.add_subplot(236)
163     ax3 = fig.add_subplot(131)
164     ax4 = fig.add_subplot(132)
165     ax5 = fig.add_subplot(133)
166     #divider1 = make_axes_locatable(ax1)
167     #cax1 = divider1.append_axes('right', size='5%', pad=0.05)
168     #divider2 = make_axes_locatable(ax2)
169     #cax2 = divider2.append_axes('right', size='5%', pad=0.05)
170     divider3 = make_axes_locatable(ax3)
171     cax3 = divider3.append_axes('right', size='5%', pad=0.05)
172     divider4 = make_axes_locatable(ax4)
173     cax4 = divider4.append_axes('right', size='5%', pad=0.05)
174     #im1=ax1.imshow(np.abs(u40), cmap='viridis', vmin=0, vmax=1)
175     #ax1.set_title('Amplitude GT')
176     #im2=ax2.imshow(np.angle(u40), cmap='twilight_shifted',vmin=-np.pi, vmax=np.pi)

```



```

5
6 import numpy as np
7 import matplotlib.pyplot as plt
8 from mpl_toolkits.axes_grid1 import make_axes_locatable
9 import cv2
10 import EasyPySpin
11
12 Cam = EasyPySpin.VideoCapture(0)
13 fig=plt.figure(0)
14 ax = fig.add_subplot(121)
15 ax1 = fig.add_subplot(122)
16 divider = make_axes_locatable(ax)
17 cax = divider.append_axes('right', size='5%', pad=0.05)
18 divider1 = make_axes_locatable(ax1)
19 cax1 = divider1.append_axes('right', size='5%', pad=0.05)
20
21 frame_nbr=0
22 while True:
23     frame_nbr+=1
24     ret, frame = Cam.read()
25     frame=cv2.flip(frame, 0)
26     frame_blurred = cv2.blur(frame, (12,12))
27     ret1, thresh = cv2.threshold(frame, 70, 255, 0)
28     thresh_blurred = cv2.blur(thresh, (12, 12))
29     im1 = ax1.imshow(thresh, cmap='gray')
30     ax1.set_title("Thresholded image")
31     M = cv2.moments(thresh_blurred)
32     cX = int(M["m10"] / M["m00"])
33     cY = int(M["m01"] / M["m00"])
34     T = np.float32([[1, 0, 1024-cX], [0, 1, 1024-cY]])
35     frame_s = cv2.warpAffine(frame, T, frame.shape)
36     im = ax.imshow(frame_s, cmap='gray')
37     ax.set_title("Sensor image")
38     scat=ax.scatter(1024,1024, color='r', marker='.')
39     scat10=ax1.scatter(1024,1024, color='r', marker='.')
40     scat11=ax1.scatter(cX,cY, color='b', marker='.')
41     scat.set_label('Sensor center')
42     scat10.set_label('Sensor center')
43     scat11.set_label('Detected centroid')
44     if frame_nbr==1:
45         ax.legend()
46         ax1.legend()
47         plt.colorbar(im, cax)
48         plt.colorbar(im1, cax1)
49     plt.pause(0.01)
50 plt.show()
51 Cam.release()
52 cv2.destroyAllWindows()

```